REPORT DOCUMENTATION PAGE

Form Approved
OMB NO. 0704-0188

1. AGENCY USE ONLY (Leave Blank)	2. REPORT DATE	3. REPORT TYPE AND DATES COVERED
	April 15, 2003	Final Report 01 July 1999-31 December 2002

4. TITLE AND SUBTITLE
Chemical Kinetic Characterization of Autoignition and Combustion of Diesel and JP-8.

5. FUNDING NUMBERS
DAAD19-99-1-0259

6. AUTHOR(S)
Dr. Kalyanasundaram Seshadri

7. PERFORMING ORGANIZATION NAME(S) AND ADDRESS(ES)
Department of Mechanical and Aerospace Engineering,
University of California at San Diego, La Jolla, California 92093-0411.

8. PERFORMING ORGANIZATION REPORT NUMBER

9. SPONSORING / MONITORING AGENCY NAME(S) AND ADDRESS(ES)
U. S. Army Research Office
P.O. Box 12211
Research Triangle Park, NC 27709-2211

10. SPONSORING / MONITORING AGENCY REPORT NUMBER
ARO Proposal Number 39886-EG.7

11. SUPPLEMENTARY NOTES
The views, opinions and/or findings contained in this report are those of the author(s) and should not be construed as an official Department of the Army position, policy or decision, unless so designated by other documentation.

12 a. DISTRIBUTION / AVAILABILITY STATEMENT
Approved for public release; distribution unlimited.

12 b. DISTRIBUTION CODE

13. ABSTRACT (Maximum 200 words)

The objective of the research was to obtain a fundamental understanding of the physical and chemical mechanisms of autoignition and combustion of diesel and JP-8 in non premixed systems. Diesel and JP-8 are comprised hundreds of aliphatic and aromatic hydrocarbon compounds. The major components of these fuels are straight chain paraffins, branched chain paraffins, cycloparaffins, aromatics, and alkenes. Detailed chemical kinetic mechanisms that describe combustion of many of the components in diesel and JP-8 are not available and are unlikely to be developed in the near future. As a consequence it is necessary to develop surrogate fuels. The research was focused on developing the necessary scientific knowledge for developing these surrogate fuels. The experimental part of the research was performed employing the counterflow configuration. The fuels tested were n-heptane, n-decane, n-dodecane, n-hexadecane, cyclohexane, methylcyclohexane, toluene, and o-xylene because they represent the types of fuels in diesel and JP-8. Critical conditions of autoignition and extinction were measured. Flame structures were measured for non premixed n-heptane flames and n-decane flames. For n-heptane and n-decane flames, numerical calculations were performed using detailed chemistry and the results were compared with experiments.

14. SUBJECT TERMS
Hydrocarbon fuels, Autoignition, Nonpremixed Flames

15. NUMBER OF PAGES
Fifty-three

16. PRICE CODE

17. SECURITY CLASSIFICATION OR REPORT	18. SECURITY CLASSIFICATION ON THIS PAGE	19. SECURITY CLASSIFICATION OF ABSTRACT	20. LIMITATION OF ABSTRACT
UNCLASSIFIED	UNCLASSIFIED	UNCLASSIFIED	UL

Enclosure 1

Chemical Kinetic Characterization of Autoignition and Combustion of Diesel and JP-8

Contents

1 Statement of the Problem Studied

The objective of the research was to obtain a fundamental understanding of the physical and chemical mechanisms of autoignition and combustion of diesel and JP-8 in non premixed systems. Experimental, numerical and analytical studies were carried out. Diesel and JP-8 comprise hundreds of aliphatic and aromatic hydrocarbon compounds. The major components of these fuels are straight chain paraffins, branched chain paraffins, cycloparaffins, aromatics, and alkenes [1–9]. A composition of diesel is given in Refs. [4] and [6] showing by volume roughly 41 % paraffins, 30 % cycloparaffins, and 29 % aromatics. The composition of diesel given in weight percent in Ref. [3] is 39 % paraffins, 44 % cycloparaffins, and 17 % aromatics. In JP-8 the concentration of paraffins is on the average 60 % by volume, that of cycloparaffins 20 %, that of aromatics 18 %, and that alkenes 2 % [1]. Detailed chemical kinetic mechanisms describing combustion for many of the components in diesel as well as those in JP-8 are not available. Therefore, an objective of this research was to develop surrogates for JP-8 and diesel. These surrogates are mixtures of several hydrocarbon compounds.

Edwards and Maurice [1] have defined two types of surrogates: physical surrogate and chemical surrogate. Physical surrogates are mixtures that have generally the same physical properties as diesel or JP-8. Physical surrogates are unlikely to reproduce aspects of combustion of diesel or JP-8. Chemical surrogates are mixtures that have generally the same chemical-class composition and average molecular weight as diesel or JP-8 [1]. In general chemical surrogates are designed to reproduce aspects of combustion of diesel or JP-8. The type of surrogate would depend on the characteristics being simulated. Edwards and Maurice [1] have suggested guidelines for developing surrogates. The objective of this study was to develop chemical surrogates that accurately reproduce autoignition and extinction characteristics of diesel and JP-8 in nonpremixed systems.

Combustion processes in diesel engines closely resemble non premixed systems. Therefore, the research was focused on non premixed flames. In non premixed systems the flow field and combustion chemistry of the fuels have a significant influence on the critical conditions of autoignition and flame extinction. Their influence can be discussed in terms of the Damköhler number, δ, defined as the ratio of a characteristic flow time, τ_f, to a characteristic chemical reaction time, τ_c. The reciprocal of the flow time can be described either by the strain rate, a, or the scalar dissipation rate, χ [10–12]. The characteristic chemical time depends on the type of fuel and the initial temperature of the reactants. Previous analytical studies on non premixed systems have shown that autoignition will take place if the value of δ is greater than some critical value δ_{I} and flame extinction will take place if the value of δ is less than some critical value δ_{e} [10–14]. Therefore for fixed τ_c, autoignition will take place for τ_f greater than some critical value or for the strain rate and the scalar dissipation rate less than some critical

value, represented by a_{I} and χ_{I}, respectively. For fixed τ_c, the flame will extinguish for τ_f less than some critical value or for the strain rate and the scalar dissipation rate greater than some critical value, represented by a_{e} and χ_{e}, respectively.

The research was performed using paraffins (*n*-heptane, *n*-decane, and *n*-dodecane) cycloparaffins (methylcyclohexane, cyclohexane), and aromatics (toluene, o-xylene) because they represent the types of fuels in diesel and JP-8. Detailed chemical kinetic mechanisms describing oxidation of a number of these compounds are either already available or they are likely to be developed. Experimental data on autoignition and flame extinction were obtained. The experimental data was used to validate detailed chemical kinetic mechanisms.

The research results are described in the journal articles 1–4, listed in section 3.1, and in the technical reports 1—10 listed in section 3.2. A number of these technical reports will be revised and submitted for publications in journals. Summaries of the results of the research are described in section 2.

2 Summary of the Most Important Results

The summaries of the important results are given in this section. The research described in sections 2.1, 2.2, 2.3, 2.5, and 2.6 are conducted on pure fuels. The results are useful for developing surrogate fuels. It has been established that that the chemical-kinetic mechanisms of oxidation of low molecular weight fuels such as hydrogen, carbon monoxide, methane, ethene (C_2H_4), ethane (C_2H_6), propene (C_3H_6), and propane (C_3H_8) are subsets of chemical-kinetic mechanisms of oxidation of *n*-heptane, *n*-decane, and *n*-hexadecane. Therefore accurate descriptions of mechanisms of oxidation of these low molecular weight fuels are necessary first steps in the development of chemical-kinetic mechanisms of oxidation of practical fuels. Accurate experimental data obtained over a wide range of conditions and different configurations are required to test the accuracies of chemical-kinetic mechanisms of combustion of various fuels. Therefore section 2.4 gives experimental data that can be used to test predictions of extinction and autoignition of chemical-kinetic mechanisms describing oxidation of C_2H_4, C_2H_6, C_3H_6, and C_3H_8. Section 2.7 describes studies leading to the development of surrogate fuels. Three body reactions, for example $H + O_2 + M \rightarrow HO_2 + M$, where M represents any third body are key steps in chemical-kinetic mechanisms of oxidation of hydrocarbon fuels. The chaperon efficiency of the third body is not well known. An experimental and numerical study focused on the influence of this reaction is described in section 2.8.

2.1 Ignition in the Viscous Layer Between Counterflowing Streams: Asymptotic Theory with Comparison to Experiments

This research is described in journal article 1 listed in section 3.1 and the report 1 listed in section 3.2. The research was performed in collaboration with Professor A. Liñán at Departamento de Motopropulsión y Termofluidodinámica, Universidad Politécnica de Madrid, Spain.

A formulation is given for describing autoignition in non premixed systems. Steady laminar flow of two counterflowing streams toward a stagnation plane is considered. One stream comprises fuel and the other oxygen. The characteristic Reynolds numbers of the counterflowing streams are presumed to be large so that the thickness of the viscous layer formed in the vicinity of the stagnation plane is small. The chemical reaction that takes place in the viscous layer between fuel and oxygen is described by a one-step overall process. The activation energy of the reaction is presumed to be large in comparison to the thermal energy. The asymptotic theory developed here makes available explicit formulas for predicting autoignition in the viscous layer. From these results a simple but reasonably accurate method is developed for deducing the activation energy, E, and frequency factor, B, of the rate of the one-step reaction between the fuel and oxygen. To illustrate the application of this method, experiments are carried out in the counterflow configuration. The fuels tested are n-heptane, n-decane, JP-10, and toluene. Experimental data obtained are the velocities and temperatures of counterflowing streams at autoignition. Values of E and B are obtained by using the experimental data in the formulas given by the asymptotic theory. These values of E and B are found to agree well with those obtained from numerical calculations.

2.2 Extinction and Autoignition of n-Heptane in Counterflow Configuration

This research is described in journal article 2 listed in section 3.1 and the report 2 listed in section 3.2. The research was performed in collaboration Dr. W. J. Pitz and Dr. H. J. Curran at Lawrence Livermore National Laboratory, Livermore, California.

A study is performed to elucidate the mechanisms of extinction and autoignition of n-heptane in strained laminar flows under non premixed conditions. A previously developed detailed mechanism made up of 2540 reversible elementary reactions among 557 species is the starting point for the study. The detailed mechanism was previously used to calculate ignition delay times in homogeneous reactors, and concentration histories of a number of species in plug-flow and jet-stirred reactors. An intermediate mechanism made up of 1282 reversible elementary reactions among 282 species and a short mechanism made up of 770 reversible elementary reactions among 160 species are assembled from this detailed mechanism. Ignition delay times in an isochoric homogeneous reactor calculated using the intermediate and the

short mechanism are found to agree well with those calculated using the detailed mechanism. The intermediate and the short mechanism are used to calculate extinction and autoignition of *n*-heptane in strained laminar flows. Steady laminar flow of two counterflowing streams toward a stagnation plane is considered. One stream made up of prevaporized *n*-heptane and nitrogen is injected from the fuel boundary and the other stream made up of air and nitrogen is injected from the oxidizer boundary. Critical conditions of extinction and autoignition given by the strain rate, temperature and concentrations of the reactants at the boundaries, are calculated. The results are found to agree well with experiments. Sensitivity analysis is carried out to evaluate the influence of various elementary reactions on autoignition. At all values of the strain rate investigated here, high temperature chemical processes are found to control autoignition. In general, the influence of low temperature chemistry is found to increase with decreasing strain. A key finding of the present study is that strain has more influence on low temperature chemistry than the temperature of the reactants.

2.3 Temperature Cross-Over and Non-Thermal Runaway at Two-Stage Ignition of N-Heptane

This research is described in journal article 3 listed in section 3.1 and the report 4 listed in section 3.2. The research was performed in collaboration with Professor N. Peters at Institut für Technische Mechanik, RWTH Aachen, 52056 Aachen, Germany.

To calculate ignition delay times a skeletal 56-step mechanism for n-heptane is further reduced to a short 30-step mechanism containing two isomers of the n-heptyl-radical and reactions describing both the high temperature and the low temperature chemistry. This mechanism reproduces ignition delay times at various pressures and temperatures reasonably well. Steady state assumptions for many of the intermediate species are introduced to derive separately two global mechanisms for the low temperature regime as well as for the intermediate and high temperature regime. In those formulations the OH radical is depleted by fast reactions with the fuel, as long as fuel is present. Its steady state relation shows that the OH concentration would blow up as soon as the fuel is depleted. Therefore the depletion of the fuel is used as a suitable criterion for ignition.

In the intermediate temperature regime the first stage ignition is related to a change from chain-branching to chain-breaking as the temperature crosses a certain threshold. The chain branching reactions result in a build-up of ketohydroperoxides which dissociate to produce OH radicals. This is associated with a slight temperature rise which leads to a crossing of the threshold temperature with the consequence that the production of OH radicals by ketohydroperoxides suddenly ceases. The subsequent second stage is driven by the much slower production of OH radicals owing to the dissociation of hydrogen peroxide. The OH radicals

react with the fuel at nearly constant temperature until the latter is fully depleted.

In all three regimes analytical solutions for the ignition delay time are presented. The reduced 4-step mechanism of the low temperature regime leads with the assumption of constant temperature to linear differential equations, which are solved. The calculated ignition delay times at fuel depletion compares well with those of the 30-step mechanism. The analysis for the intermediate temperature regime starts from a 4-step subset of a 9-step reduced mechanism. It contains the cross-over dynamics in form of a temperature dependent stoichiometric coefficient which is analyzed mathematically. The resulting closed form solutions describe the first stage ignition, the temperature cross-over and the second stage ignition. They also identify the rate determining reactions and quantify the influence of their rates on the first and the second ignition times. The high temperature regime is governed by a three-step mechanism leading to a nonlinear problem which is solved by asymptotic analysis.

While the dissociation reaction of the ketohydroperoxide dominates the low temperature regime and the first stage ignition of the intermediate temperature regime, the hydrogen peroxide dissociation takes this role for the second stage of the intermediate and in the high temperature regime. The overall activation energy of the ignition delay time in the low temperature regime is the mean of the activation energies of two reactions only. The overall activation energy of the ignition delay time in the high temperature regime is shown to be related to the activation energies of only three but different rate determining reactions.

2.4 Nonpremixed and Premixed Extinction and Autoignition of C_2H_4, C_2H_6, C_3H_6, and C_3H_8

This research is described in journal article 4 listed in section 3.1 and report 3 and report 6 listed in section 3.2.

Experimental studies are conducted on laminar nonpremixed and premixed flames stabilized in the counterflow configuration. The fuels tested are ethene (C_2H_4), ethane (C_2H_6), propene (C_3H_6), and propane (C_3H_8). Studies on nonpremixed systems are carried out by injecting a fuel stream made up of fuel and nitrogen (N_2) from one duct and an oxidizer stream made up of air and N_2 from the other duct. Studies on premixed systems are carried out by injecting a premixed reactant stream made up of fuel, oxygen, and nitrogen from one duct, and an inert-gas stream of N_2 from the other duct. Critical conditions of extinction are measured by increasing the flow rates of the counterflowing streams until the flame extinguishes. Critical conditions of autoignition are measured by preheating the oxidizer stream of the non premixed system and the inert-gas stream of the premixed system. Experimental data for autoignition are obtained over a wide range of temperatures of the heated streams. In

addition for premixed systems experimental data are obtained for a wide range of values of the equivalence ratio including fuel-lean and fuel-rich conditions. Numerical calculations are performed using a detailed chemical-kinetic mechanism and compared with measurements. The present study highlights the influences of nonuniform flow field on autoignition in premixed systems that were not available from previous studies using shock tubes. For the premixed system considered here the changes in the strain rates at extinction with equivalence ratio are found to be similar to previous observations of changes in laminar burning velocities with equivalence ratio. The studies on autoignition in the premixed system show that the temperature of the inert-gas stream at autoignition reaches a minimum for a certain equivalence ratio. For premixed systems abrupt extinction and autoignition are not observed if the value of the equivalence ratio is less than some critical value.

2.5 Chemical Kinetic Study of Toluene Oxidation

This research is described in report 5 and report 7 listed in section 3.2. The research was performed in collaboration with W. J. Pitz and C. K. Westbrook at Lawrence Livermore National Laboratory, Livermore, California, J. W. Bozzelli, and C.-J. Chen, at Chemistry and Chemical Engineering Department, New Jersey Institute of Technology, Newark, NJ, and I. Da Costa, R. Fournet, F. Billaud, F. Battin-Leclerc, at Département de Chime Physique des Réactions, CNRS-ENSIC, BP. 451, 1, rue Grandville, 51001 Nancy, France.

A study was performed to elucidate the chemical-kinetic mechanism of combustion of toluene. A detailed chemical-kinetic mechanism for toluene was improved by adding a more accurate description of the phenyl + O_2 reaction channels, toluene decomposition reactions and the benzyl + O reaction. Results of the chemical kinetic mechanism are compared with experimental data obtained from premixed and non premixed systems. Under premixed conditions, predicted ignition delay times are compared with new experimental data obtained in shock tube. Also, calculated species concentration histories are compared to experimental flow reactor data from the literature. Under non premixed conditions, critical conditions of extinction and autoignition were measured in strained laminar flows in the counterflow configuration. Numerical calculations are performed using the chemical-kinetic mechanism at conditions corresponding to those in the experiments. Critical conditions of extinction and autoignition are predicted and compared with the experimental data. Comparisons between the model predictions and experimental results of ignition delay times in shock tube, and extinction and autoignition in non premixed systems show that the chemical-kinetic mechanism predicts that toluene/air is overall less reactive than observed in the experiments. For both premixed and non premixed systems, sensitivity analysis was used to identify the reaction rate constants that control the overall rate of oxidation in each of the systems considered. Under shock tube conditions, the reactions that influence ignition delay time are H + O_2

chain branching, the toluene decomposition reaction to give an H atom, and the toluene + H abstraction reaction. The reactions that influence autoignition in non premixed systems involve the benzyl + HO_2 reaction and the phenyl + O_2 reaction.

Further details of this work is given in Appendix A. A journal publication describing results of this research is under preparation.

2.6 The Structure of Nonpremixed *n*-Decane Flames

This research is described in report 8 listed in section 3.2.

An experimental and numerical study is performed to elucidate the structure and mechanisms of extinction and autoignition *n*-decane flames in strained laminar flows under nonpremixed conditions. Experiments are conducted on flames stabilized between two counterflowing streams. The fuel-stream is a mixture of prevaporized *n*-decane and nitrogen, and the oxidizer stream is a mixture of air and nitrogen. Concentration profiles of $C_{10}H_{22}$, O_2, N_2, CO_2, CO, H_2O, CO, CH_4, C_2-hydrocarbons, C_3-hydrocarbons, and C_4-hydrocarbons, are measured. The measurements are made by removing gas samples from the flame using a quartz microprobe and analyzing the samples using a gas chromatograph. Temperature profiles are measured using a thermocouple. Numerical calculations are performed using detailed chemistry to determine the flame structure and the results are compared with the measurements. Critical conditions of extinction are measured. Data giving the mass fraction of oxygen in the oxidizer stream as a function of the strain rate at extinction are obtained. Critical conditions of autoignition are measured. Data giving the temperature of the oxidizer stream as a function of the strain rate are obtained. Numerical calculations are performed using detailed chemistry. Critical conditions of extinction and autoignition are obtained and compared with measurements.

Further details of this work is given in Appendix B. A journal publication describing results of this research is under preparation.

2.7 Autoignition and Extinction of Hydrocarbon Fuels in Nonpremixed Systems

This research is described in report 9 listed in section 3.2.

Experimental studies are carried out on extinction and autoignition of liquid hydrocarbon fuels in nonpremixed systems. The counterflow configuration is employed. In this configuration an oxidizer made up of air and nitrogen flows over the surface of a pool of liquid fuel.

Critical conditions of extinction are measured for *n*-heptane, *iso*-octane, *n*-octane, *n*-decane, *n*-dodecane, *n*-hexadecane, methylcyclohexane, cyclohexane, diesel and JP-8. Data giving the mass fraction of oxygen in the oxidizer stream as a function of the strain rate at extinction are obtained. Critical conditions of autoignition are measured for *n*-heptane, *iso*-octane, *n*-octane, *n*-decane, *n*-dodecane, *n*-hexadecane, methylcyclohexane, *o*-xylene, JP-10, diesel and JP-8. The experimental results show that the critical conditions of extinction of *iso*-octane, hexadecane, and a mixture of 70 % decane and 30 % xylene are similar to that of diesel/ The critical conditions of autoignition, however, of these fuels and fuel mixture are not similar to that of diesel. This illustrates the challenges in developing surrogate fuels.

Further details of this work is given in Appendix C. A journal publication describing results of this research is under preparation.

2.8 The Influence of Water Vapor of the Critical Conditions of Extinction and Autoignition of Premixed Ethene Flames

This research is described in report 10 listed in section 3.2.

An experimental and numerical study is performed to elucidate the influence of addition of water vapor on the structure and mechanisms of extinction and autoignition premixed ethene (C_2H_4) flames in strained laminar flows. Experiments are conducted on flames stabilized between two counterflowing streams. The counterflow burner is made up of two ducts. A premixed reactant stream made up of C_2H_4, air, and nitrogen is injected from one duct, and an inert gas stream of N_2 is injected from the other duct. Water vapor is added to the premixed reactant stream using a vaporizer. The vaporizer contains liquid water that is heated using an electrical heater. The temperature of water is measured using a thermocouple. The water-vapor in the vaporizer is presumed to be in equilibrium with the liquid. A part of the air in premixed reactant stream percolates through the liquid water in the vaporizer. The mass fraction of water vapor in the premixed reactant stream, Y_{H_2O}, can be changed either by changing the temperature of the water in the vaporizer or the flow rate of air through the vaporizer. The premixed reactant stream is characterized by the equivalence ratio ϕ and the adiabatic temperature T_{ad}. To clarify the influence of water vapor on extinction and autoignition studies are carried out at fixed values of ϕ and T_{ad}. Critical conditions of extinction are measured by increasing the flow rates of the counterflowing streams until the flame extinguishes. Critical conditions of autoignition are measured by preheating the inert gas stream of the premixed system. Experimental data are obtained for a wide range of values of Y_{H_2O}. Numerical calculations are performed using a detailed chemical kinetic mechanism and compared with measurements.

Further details of this work is given in Appendix D. A journal publication describing results of this research is under preparation.

3 List of all Publications and Technical Reports

3.1 Journal Articles

1. Seiser, R., Seshadri, K., Piskernik, E., and Liñán, A., "Ignition in the Viscous Layer Between Counterflowing Streams: Asymptotic Theory with Comparisons to Experiments" *Combustion and Flame,* **122**, 2000, pp 339–349.

2. Seiser, R., Pitsch, H., Seshadri, K., Pitz, W. J., Curran, H. J., "Extinction and Autoignition of *n*-Heptane in Counterflow Configuration," *Proceedings of the Combustion Institute,* **28**, 2000, pp 2029-2037.

3. Peters, N., Paczko, G., Seiser, R., and Seshadri, K., "Temperature Cross-Over and Non-Thermal Runway at the Two-Stage Ignition of N-Heptane," *Combustion and Flame,* **128**, 2002, pp 38–59.

4. Humer, S., Seiser, R., and Seshadri, K., "Nonpremixed and Premixed Extinction and Autoignition of C_2H_4, C_2H_6, C_3H_6, and C_3H_8," *Proceedings of the Combustion Institute,* **29**, 2002, accepted for publication.

3.2 Papers Published in Proceedings of Technical Meetings

1. R. Seiser, K. Seshadri, E. Piskernik, and A. Liñán, "Ignition in the Viscous layer Between Counterflowing Streams: Asymptotic Theory with Comparison to Experiments," Paper # 00S-27, Western States Section of the Combustion Institute, Spring 2000 Meeting, Colorado School of Mines, Golden, CO 80401, March 13—14, 2000.

2. R. Seiser, H. Pitsch, K. Seshadri, W. J. Pitz, and H. J. Curran, "Extinction and Autoignition of *n*-Heptane in Counterflow Configuration," Paper # 00S-28, Western States Section of the Combustion Institute, Spring 2000 Meeting, Colorado School of Mines, Golden, CO 80401, March 13—14, 2000.

3. R. Seiser, K. Seshadri, and W. J. Pitz, "Experimental and Numerical Studies of Extinction and Autoignition of C_3H_8, C_3H_6, C_2H_6, and C_2H_4," paper # 149, 2^{nd} Joint Meeting of the US Sections of the Combustion Institute, Oakland California, March 25—28, 2001.

4. N. Peters, G. Paczko, R. Seiser, and K. Seshadri, "Temperature Cross-Over and Non-Thermal Runaway at Two-Stage Ignition of *n*-Heptane," paper # 146, 2^{nd} Joint Meeting of the US Sections of the Combustion Institute, Oakland California, March 25—28, 2001.

5. W. J. Pitz , C. K. Westbrook, R. Seiser, K. Seshadri, J. W. Bozzelli, I. Da Costa, R. Fournet, F. Billaud, and F. Battin-Leclerc, "Chemical-Kinetic Characterization of Combustion of Toluene," "Chemical-Kinetic Study of Toluene Oxidation," paper # 252, 2^{nd} Joint Meeting of the US Sections of the Combustion Institute, Oakland California, March 25—28, 2001.

6. S. Humer , R. Seiser, and K. Seshadri, "Counterflow Ignition of Premixed Ethene/Air Mixtures with Heated Nitrogen," paper # 01F-6, Western States Section of the Combustion Institute, Fall 2001 Meeting, University of Utah, Salt Lake City, Utah, October 15—16, 2001.

7. W. J. Pitz, R. Seiser, J. W. Bozzelli, I. Da Costa, R. Fournet, F. Billaud, F. Battin-Leclerc, K. Seshadri, and C. K. Westbrook, "Chemical-Kinetic Study of Toluene Oxidation," paper # 01F-28, Western States Section of the Combustion Institute, Fall 2001 Meeting, University of Utah, Salt Lake City, Utah, October 15—16, 2001.

8. Tanoue, K., Seiser, R., and Seshadri, K., "The Structure of Nonpremixed *n*-Decane Flames," Paper A31, 3^{rd} Joint Meeting of the United States Sections of the Combustion Institute, The University of Illinois at Chicago, Chicago, March 16–19, 2003.

9. Humer, S., Seiser, R. , and Seshadri, K., "Autoignition and Extinction of Hydrocarbon Fuels in Nonpremixed Systems," Paper B26, 3^{rd} Joint Meeting of the United States Sections of the Combustion Institute, The University of Illinois at Chicago, Chicago, March 16–19, 2003.

10. Geieregger, M., Seiser, R., and Seshadri, K., "The Influence of Water Vapor on the Critical Conditions of Extinction and Autoignition pf Premixed Ethene Flames," Paper B27, 3^{rd} Joint Meeting of the United States Sections of the Combustion Institute, The University of Illinois at Chicago, Chicago, March 16–19, 2003.

4 Participating Scientific Personnel

The participating scientific personnel were 1) Professor K. Seshadri, 2) Dr. R. Seiser (research staff), 3) Dr. K. Tanoue (visiting scholar), 4) Mr. S. Humer (graduate student), 5) Mr. E. Piskernick (graduate student), and 6) M. Geieregger (graduate student).

5 Report of Inventions

None.

References

[1] T. Edwards and L. Q. Maurice. Surrogate mixtures to represent complex aviation and rocket fuels. *Journal of Propulsion and Power*, 17:461–466, 2001.

[2] T. Edwards. "Real" kerosene aviation and rocket fuels: Compositions and surrogates. *2001 Fall Technical Meeting, Eastern States Section of the Combustion Institute*, 2001.

[3] C. Pereira, J-M Bae, S. Ahmed, and M. Krumpelt. Liquid fuel reformer development: Autothermal reforming of diesel fuel. *Proceedings of the 2000 Hydrogen Program Review*, NREL/CP-570-28890, 2000.

[4] P. Flynn. Concentration of various hydrocarbon compounds in diesel. Cummins, private communication, 1998.

[5] L. Q. Maurice. *Detailed Chemical Kinetic Models for Aviation Fuels*. Ph.D thesis, The University of London, 1996.

[6] H. Wenck und C. Schneider. DGMK-Projekt 409: Chemisch-physikalische Daten von Otto-und Dieselkraftstoffen. Technical report, DGMK Deutsche wissenschaftliche Gesellschaft für Erdöl, Erdgas und Kohle E. V., Hamburg, November 1993.

[7] S. P. Heneghan, S. L. Locklear, D. L. Geiger, S. D. Anderson, and W. D. Schulz. Static tests of jet fuel thermal and oxidative stability. *AIAA, Journal of Propulsion and Power*, 9:5–9, 1993.

[8] Handbook of aviation fuel properties. CRC Report No. 530, Coordinating Research Council, Inc, Atlanta, Georgia, 1988.

[9] Jet fuel specifications. Exxon Company, International Marketing Department, 1995.

[10] A. Liñán. The asymptotic structure of counterflow diffusion flames for large activation energies. *Acta Astronautica*, 1:1007–1039, July 1974.

[11] N. Peters. Local quenching due to flame stretch and non-premixed turbulent combustion. *Combustion Science and Technology*, 30:1–17, 1983.

[12] N. Peters. Laminar diffusion flamelet models in non-premixed turbulent combustion. *Progress in Energy and Combustion Science*, 10:319–339, 1984.

[13] F. A. Williams. *Combustion Theory*. Addison-Wesley Publishing Company, Redwood City, CA, 2 edition, 1985.

[14] A. Liñán and F. A. Williams. *Fundamental Aspects of Combustion*, volume 34 of *Oxford Engineering Science Series*. Oxford University Press, New York, 1993.

[15] A. Violi, S. Yan, E. G. Eddings, A. F. Sarofim, S. Granata, T. Faravelli, and E. Ranzi. Experimental formulation and kinetic model for JP-8 surrogate mixtures. *Combustion Science and Technology*, 174:399–417, 2002.

Appendix A: Chemical Kinetic Study of Toluene Oxidation

W. J. Pitz[1], R. Seiser[2], J. W. Bozzelli[3], K. Seshadri[2], C.-J. Chen[3], I. Da Costa[4], R. Fournet[4], F. Billaud[4], F. Battin-Leclerc[4], and C. K. Westbrook[1]

[1]Lawrence Livermore National Laboratory, P. O. Box 808, Livermore, California 94551, USA
[2] Department of Mechanical and Aerospace Engineering, University of California at San Diego, La Jolla, California 92093-0411, USA
[3] Chemistry and Chemical Engineering Department, New Jersey Institute of Technology, Newark, NJ 07102, USA
[4] Département de Chime Physique des Réactions, CNRS-ENSIC, BP. 451, 1, rue Grandville, 51001 Nancy, France.

Abstract

A study was performed to elucidate the chemical-kinetic mechanism of combustion of toluene. A detailed chemical-kinetic mechanism for toluene was improved by adding a more accurate description of the phenyl + O_2 reaction channels, toluene decomposition reactions and the benzyl + O reaction. Results of the chemical kinetic mechanism are compared with experimental data obtained from premixed and nonpremixed systems. Under premixed conditions, predicted ignition delay times are compared with new experimental data obtained in shock tube. Also, calculated species concentration histories are compared to experimental flow reactor data from the literature. Under nonpremixed conditions, critical conditions of extinction and autoignition were measured in strained laminar flows in the counterflow configuration. Numerical calculations are performed using the chemical-kinetic mechanism at conditions corresponding to those in the experiments. Critical conditions of extinction and autoignition are predicted and compared with the experimental data. Comparisons between the model predictions and experimental results of ignition delay times in shock tube, and extinction and autoignition in nonpremixed systems show that the chemical-kinetic mechanism predicts that toluene/air is overall less reactive than observed in the experiments. For both premixed and nonpremixed systems, sensitivity analysis was used to identify the reaction rate constants that control the overall rate of oxidation in each of the systems considered. Under shock tube conditions, the reactions that influence ignition delay time are H + O_2 chain branching, the toluene decomposition reaction to give an H atom, and the toluene + H abstraction reaction. The reactions that influence autoignition in nonpremixed systems involve the benzyl + HO_2 reaction and the phenyl + O_2 reaction.

Introduction

Alkylated benzenes are an important class of hydrocarbons because they comprise a significant portion of gasoline and diesel fuels. Knowledge of the oxidation chemistry of alkylated

benzenes is needed in developing predictive models that can treat autoignition, and premixed and nonpremixed burning of transportation fuels in internal combustion engines. Toluene ($C_6H_5CH_3$) has one of the simplest molecular structures of the alkylated benzenes and is a reasonable starting point for the development of detailed chemical-kinetic reaction mechanisms for alkylated benzenes. Much previous work has been done on the oxidation of toluene. Several research groups have developed detailed chemical-kinetic reaction mechanisms for toluene. Most recently, Klotz et al. [1] supplemented the toluene mechanism of Emdee et al. [2] to improve the predictions for the intermediates 1,3 butadiene, acetylene and benzaldehyde. Zhong and Bozzelli [3–5] developed a more accurate description of radical additions to cyclopentadiene and associations with cyclopentadienyl radical; they included these reactions in a detailed chemical-kinetic mechanism for toluene that they developed. Lindstedt and Maurice [6] developed a very comprehensive toluene mechanism whose predictions they compared to experimental results from counterflow diffusion flames, plug flow reactors, shock tubes and premixed flames. Emdee et al. [2] developed a detailed chemical-kinetic mechanism for toluene that was benchmark for many years.

There are quite a few experimental studies of toluene oxidation whose data are very useful for mechanism validation. Several experimental studies of toluene oxidation in a flow reactor were performed at Princeton University [1, 2, 7, 8]. Ignition of toluene in a rapid compression machine was performed by Griffiths et al. [9] and by Roubaud et al. [10]. Their rapid compression machine results show that toluene oxidation chemistry lacks the two stage ignition observed in paraffinic fuels. Experimental data for the critical conditions of autoignition of toluene in the counterflow configuration are given in Ref. [11]. Using this experimental data, overall chemical-kinetic rate parameters that characterize the rate of one-step overall reaction between fuel and oxygen were obtained [11]. The present work offers new results for shock tube ignition of toluene and new results for extinction under nonpremixed conditions. These experiments provide additional data for validating chemical-kinetic mechanisms for toluene. In particular, the results under nonpremixed conditions highlight the influence of strain on autoignition and extinction.

Experimental

Shock tube experiments

The experiments were performed in a stainless steel 78 mm diameter shock tube at DCPR-CNRS-NANCY. The reaction and driver parts were separated by two terphane diaphragms, which were ruptured by suddenly decreasing the pressure in the space separating them. The driver gas was helium and the reacting mixture was diluted in argon. The incident and reflected shock velocities were measured by four piezo-electric pressure transducers located along

the reaction section. The state of the test gas behind the incident and the reflected shock waves was derived from the value of the incident shock velocity by using classical, one-dimensional, shock equations of mass, momentum, and energy conservation applied to an ideal gas.

The pressure profile displayed three rises, which were due to the incident shock wave, the reflected shock wave and the ignition, respectively. The onset of ignition was, however, most accurately detected by OH radical emission at 306 nm through a quartz window with a photomultiplier fitted with a monochromator at the end of the reaction section. The last pressure transducer was located at the same place along the axis of the tube as the quartz window. The ignition delay time was defined as the time interval between the pressure rise measured by the last pressure transducer due to the arrival of the reflected shock wave and the rise of the optical signal by the photomultiplier up to 10 % of its maximum value. The ignition delay times were corrected for blast wave effects by adding 3 μs to the measured time [12].

Oxygen and helium were purchased from Air Liquide-Alphagaz and toluene was provided by Aldrich (purity: 99.8 %). The toluene concentration in the reactants was kept constant at 1.25 %. The values of equivalence ratio, ϕ, examined were 0.5, 1.0 and 1.5. The reflected shock pressures and temperatures ranged from 8.0 to 9.4 atm and 1300 to 1900 K, respectively.

Experiments under Nonpremixed Conditions

Experiments under nonpremixed conditions were carried out in the counterflow configuration. Figure 1 shows a schematic illustration of the counterflow configuration. Steady, axisymmetric, laminar flow of two counterflowing streams toward a stagnation plane is considered. In this configuration a fuel stream made up of prevaporized toluene and nitrogen is injected from the fuel-duct, and an oxidizer stream of air is injected from the oxidizer-duct. These jets flow into the mixing layer between the two ducts. The exit of the fuel-duct is called the fuel boundary and the exit of the oxidizer-duct the oxidizer boundary. The mass fraction of fuel, the temperature, and the component of the flow velocity normal to the stagnation plane at the fuel boundary are represented by $Y_{\mathrm{F},1}$, T_1, and V_1, respectively. The mass fraction of oxygen, the temperature, and the component of the flow velocity normal to the stagnation plane at the oxidizer boundary are represented by $Y_{\mathrm{O}_2,2}$, T_2, and V_2, respectively. The tangential components of the flow velocities at the boundaries are presumed to be equal to zero. The distance between the fuel boundary and the oxidizer boundary is represented by L.

In the experiments the momenta of the counterflowing reactant streams $\rho_i V_i^2, i = 1, 2$ at the boundaries are kept equal to each other. Here ρ_1 and ρ_2 represent the density of the mixture at the fuel boundary and at the oxidizer boundary, respectively. This condition ensures that the stagnation plane formed by the two streams is approximately in the middle

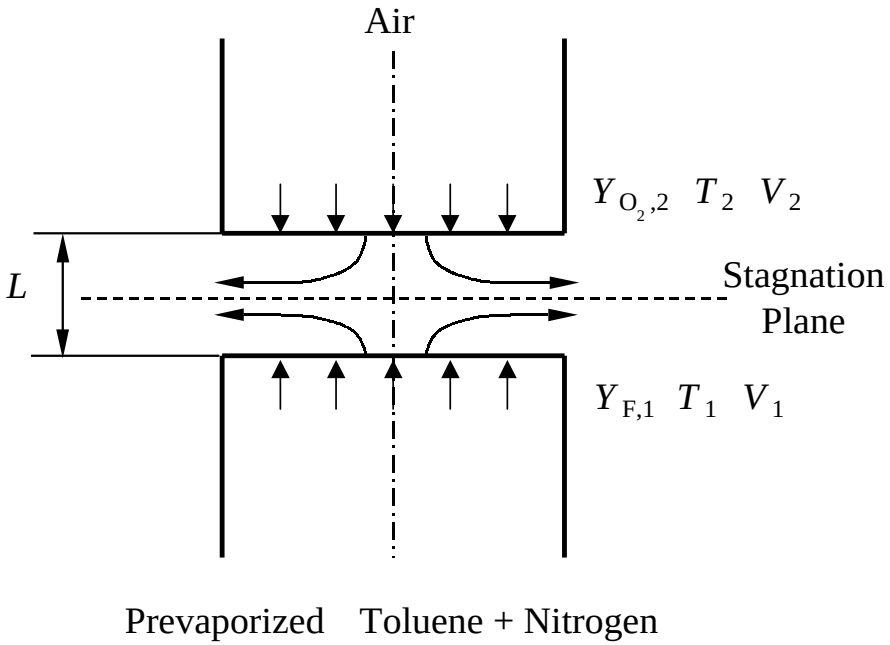

Figure 1: Schematic illustration of the counterflow configuration.

of the region between the two boundaries. The value of the strain rate, defined as the normal gradient of the normal component of the flow velocity, changes from the fuel boundary to the oxidizer boundary [13]. The characteristic strain rate on the oxidizer side of the stagnation plane a_2 is presumed to be given by [13]

$$a_2 = \frac{2|V_2|}{L}\left(1 + \frac{|V_1|\sqrt{\rho_1}}{|V_2|\sqrt{\rho_2}}\right). \tag{1}$$

Equation 1 is obtained from an asymptotic theory where the Reynolds numbers of the laminar flow at the boundaries are presumed to be large [13]. Critical conditions of extinction are presumed to be given by the strain rate, $a_{2,e}$, and the mass fraction of fuel at the fuel boundary. Critical conditions of autoignition are presumed to be given by the strain rate, $a_{2,I}$, the temperature of the oxidizer stream, $T_{2,I}$, and the mass fraction of fuel and at the fuel boundary. The experiments were conducted at a pressure of 1.013 bar.

A detailed description of the burner is given elsewhere [11, 14]. The flow rates of gases were measured by computer-regulated mass flow controllers. The velocities of the reactants at the boundaries were presumed to be equal to the ratio of their volumetric flowrates to the cross-section area of the ducts. The temperature of the fuel stream and the temperature of the oxidizer stream at the boundaries were measured using thermocouples. The measured

temperatures were corrected for radiative heat losses. The accuracy of the radiation-corrected temperatures is expected to be $\pm 25\,\mathrm{K}$. A brief description of the experimental procedure is given here.

In the extinction experiments the temperature of the fuel stream, $T_1 = 378\,\mathrm{K}$, and the temperature of the oxidizer stream, $T_2 = 298\,\mathrm{K}$. The distance between the fuel boundary and the oxidizer boundary was $L = 10\,\mathrm{mm}$. At some selected value of $Y_{\mathrm{F},1}$ the flame was stabilized at $a_2 < a_{2,e}$. The strain rate was increased by increasing V_1 and V_2 until extinction was observed. Experimental results are shown later. Previous autoignition experiments were conducted with the mole fraction of prevaporized fuel maintained at 0.15 [11]. The temperature at the fuel boundary, $T_1 = 378\,\mathrm{K}$. The distance between the fuel boundary and the oxidizer boundary was $L = 12\,\mathrm{mm}$. At a given strain rate and oxidizer temperature $T_2 < T_{2,I}$ the flow field was established. The temperature at the oxidizer boundary was gradually increased until autoignition took place. Experimental results are shown later.

Detailed Chemical-Kinetic Mechanism

The detailed chemical-kinetic mechanism for toluene was assembled by adding the toluene and benzene reaction mechanism of Zhong et al. [2–5] to the C_1-C_4 mechanism of Refs. [15] and [16]. The detailed chemical-kinetic mechanism is made up 349 species and 1631 reversible reactions. The entire mechanism will be available from our Web page (see Ref. [17]). The ultimate objective of this work is to add toluene as a fuel component to detailed chemical-kinetic mechanisms for alkanes that have been developed at Lawrence Livermore National Laboratories (LLNL) [18]. This combined alkane-toluene mechanism will provide a more complete mechanism for modeling combustion of gasoline or diesel fuels.

The toluene mechanism was improved in several ways. Rate constants of key reactions were estimated using Quantum RRK analysis to obtain $k(E)$ and master equation analysis [19] to evaluate pressure fall-off. Reactions analyzed included toluene decomposition reactions and the reaction of benzyl radicals with O atoms. The unimolecular decomposition of toluene giving benzyl + H was found to be an important reaction controlling shock tube ignition. The reaction of benzyl radicals with O atoms to give benzyaldehyde + H is the primary path consuming benzyl under shock tube and flow reactor conditions.

The reaction rate constants for phenyl + O_2 system developed by Bozzelli et al. [19] were incorporated. These reaction channels included new products for which consumption reactions were added. The phenyl + O_2 rate constants were found to play an important role under counterflow-ignition conditions.

The rate constant for the initiation reaction (toluene + $O_2 \rightleftharpoons$ benzyl + HO_2) was updated ($k = 9.3\times10^8\, T^{1.301} \exp(-40939.0\,\mathrm{cal}/RT)\,\mathrm{cm}^3/(\mathrm{mol\cdot s})$) using one half the rate constant of allylic isobutene + O_2 [20]. Our estimate is 50 percent higher than the estimate of Walker [21] at 1000 K. Reactions to consume bicyclopentadiene were also added.

Comparisons between Numerical Calculations and Experiments

Shock Tube Comparisons

The ignition in the shock tube was simulated using the Senkin code [22] assuming constant volume combustion after the reflected shock passes through the mixture. The measured results are compared to predicted results in Fig. 2. In the experiments, 10 percent of the maximum

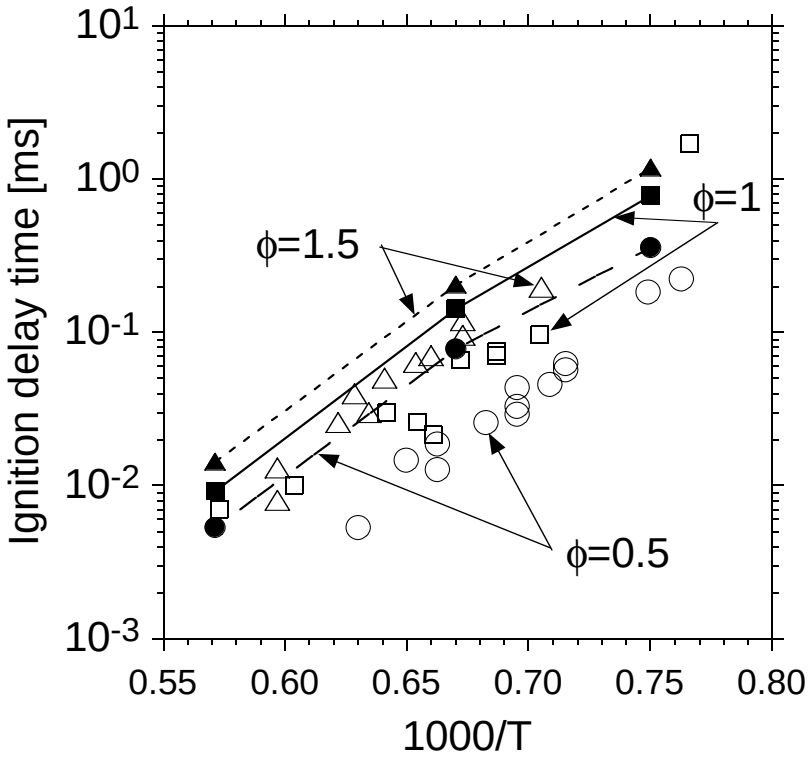

Figure 2: Predicted (lines and filled symbols) and measured (unfilled symbols) ignition delay times of toluene/O_2/Ar mixtures under shock tube conditions. (T = reflected shock temperature in Kelvin).

OH emission was used as an indication of ignition. The computed ignition delay time was obtained using the inflection in the temperature profile as an indication of ignition. When 10 percent of the OH maximum concentration was used in the calculations, almost identical

results were obtained over the temperature range considered. We did not attempt to simulate OH emission. The predicted ignition delay times compared reasonably well with experimental values for the fuel-rich case, but were too long for the fuel-lean case.

Standard Senkin sensitivity analysis [22] was performed to determine the reaction rate constants that control the oxidation of toluene under shock tube conditions. The Senkin code gives the change in species concentration for an incremental change in reaction rate constant. The OH radical concentration was chosen as an indicator of the overall reactivity of the system. An alternate choice of toluene concentration produced similar results. The sensitivity of OH concentration to a change in reaction rate constant is shown in in Fig. 3. The results are

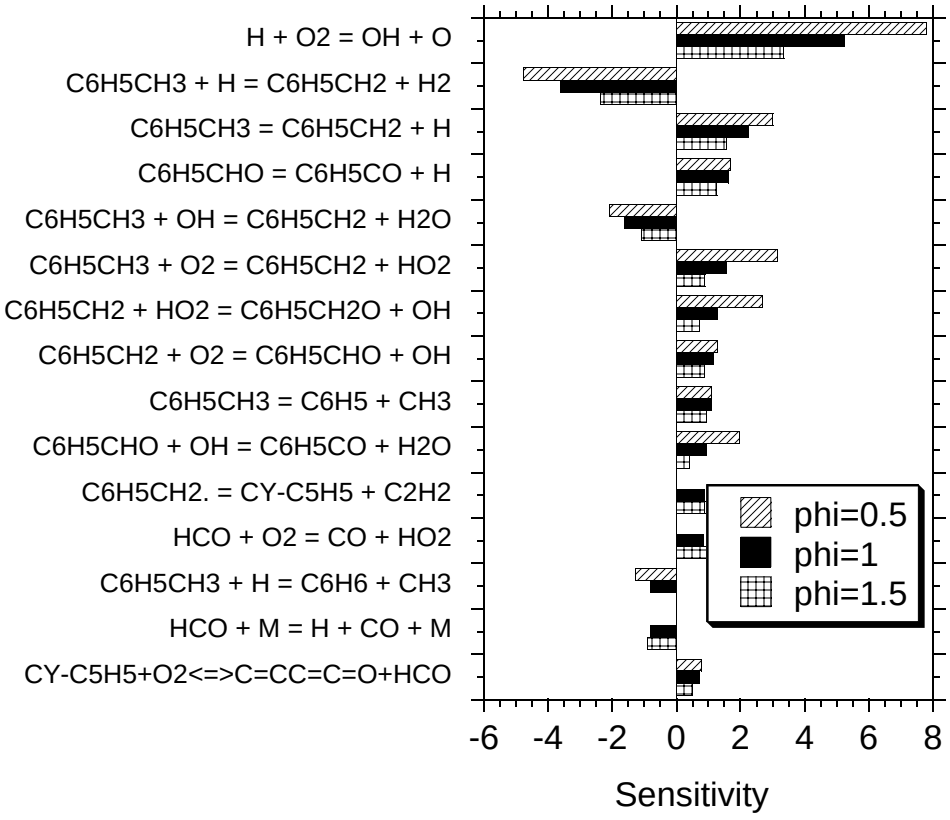

Figure 3: Sensitivity of the OH radical concentration to changes in individual rate constants under the shock tube conditions shown in Fig. 2 with $1000/T = 0.67$, where T is given in Kelvin.

shown when the toluene is about half consumed. Positive sensitivities indicate, an increase in rate constant increases the OH concentration and accelerates the overall rate of reaction, while negative sensitivities indicate an increase in rate constant decreases the OH concentration and retards the overall rate of reaction. The reaction giving the highest sensitivity is H + O_2 chain

branching (Fig. 3). The sensitivities of the other controlling reactions can be understood in relationship to it. The abstraction reaction

$$C_6H_5CH_3 + H = C_6H_5CH_2\cdot + H_2,$$

removes H atoms that would otherwise lead to chain branching via H + O_2 so it exhibits a high negative sensitivity and retards ignition. We used the rate constant from Baulch et al. [23]. This rate constant has an uncertainty of about a factor of 2 at 1700 K. The toluene decomposition channel,

$$C_6H_5CH_3 = C_6H_5CH_2\cdot + H,$$

produces H atoms that can then lead to chain branching and thus exhibits a high positive sensitivity and accelerates ignition. This reaction was analyzed carefully with quantum RRK and master equation treatment because of its importance under shock tube conditions. The reaction $C_6H_5CHO = C_6H_5CO\cdot$ + H also produces H atoms and therefore exhibits a significant positive sensitivity. The inclusion of this reaction significantly improved the shock tube predictions at high temperature. The reaction of toluene with OH shows a large negative sensitivity and thus retards ignition. At fuel-lean conditions, the reaction $C_6H_5CH_3 + O_2 = C_6H_5CH_2\cdot + HO_2$ shows a high positive sensitivity. Further theoretical or experimental investigations of this reaction and the reaction of toluene with H atoms may help improve agreement with the shock tube experiments under fuel-lean conditions.

Flow Reactor Comparisons

The flow reactor was simulated using the Senkin code [22]. The predicted results are compared to the measurements of Klotz et al. [1] in Figs. 4 and 5. The results of the fuel profile look reasonable and the early appearance of the benzylaldehyde peak compared to the benzene peak is predicted. Many of the peak intermediate concentrations are predicted within a factor of two of the measurements, except for benzyladehyde which is within a factor of three and 1,3-butadiene which is predicted to be in very low concentrations compared to the measurements.

Senkin sensitivity analysis [22] was performed to determine the reaction rate constants that control the oxidation of toluene under flow reactor conditions. The toluene concentration was chosen as an indicator of the overall reactivity of the system. The sensitivity of the toluene concentration at 135 ms to a change in reaction rate constant is shown in Fig. 6. At 135 ms, the initial toluene is about 48 percent consumed. Negative sensitivities indicate that the reaction accelerates the overall rate of reaction and positive sensitivities indicate the opposite effect. The reaction exhibiting the highest sensitivity is again the H + O_2 chain branching reaction. The second most sensitive reaction is the reaction of benzyl and O_2:

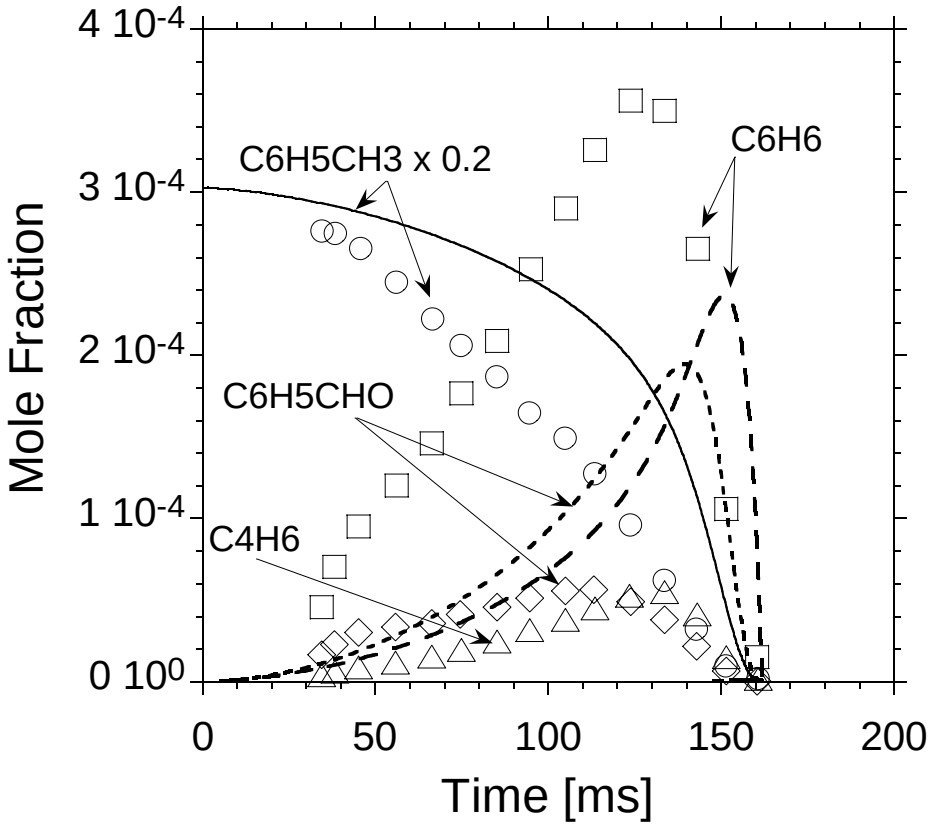

Figure 4: Predicted and measured concentration histories under flow reactor conditions. ($\phi =$ 0.76, N_2 98 %, initial temperature = 1173 K, atmospheric pressure, time is residence time in flow reactor). The symbols represent measurements of Klotz et al. [1]. The lines are results of numerical calculations.

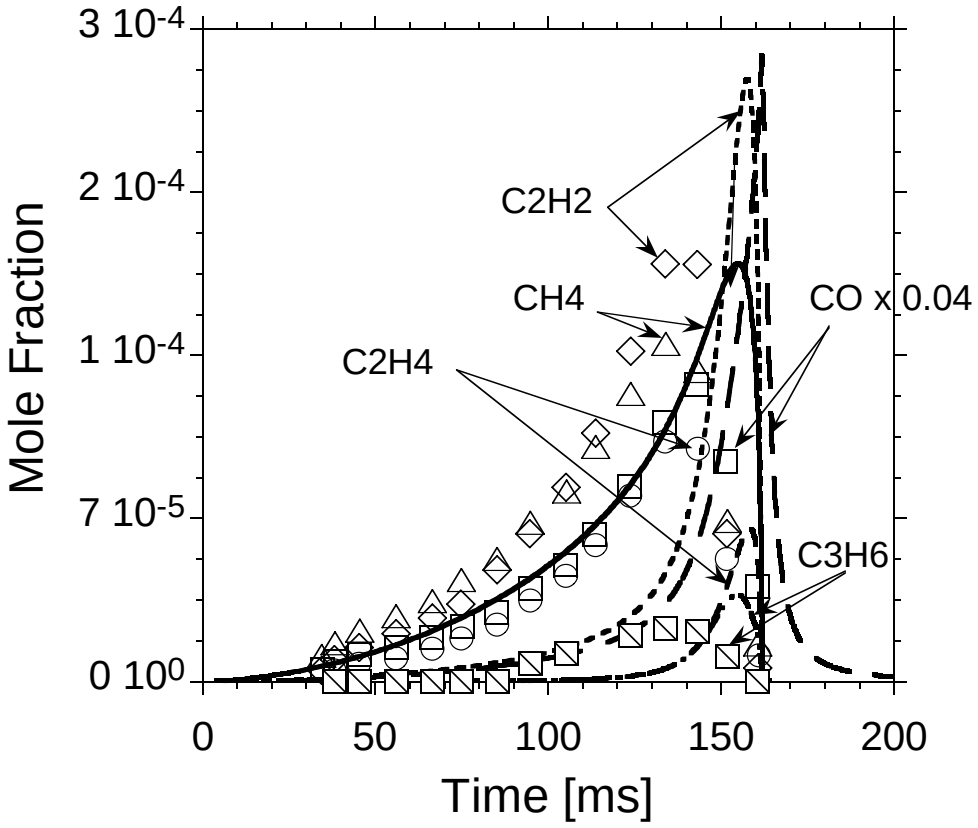

Figure 5: Predicted and measured concentration histories under flow reactor conditions. ($\phi =$ 0.76, N_2 98 %, initial temperature = 1173 K, atmospheric pressure, time is residence time in flow reactor). The symbols represent measurements of Klotz et al. [1]. The lines are results of numerical calculations.

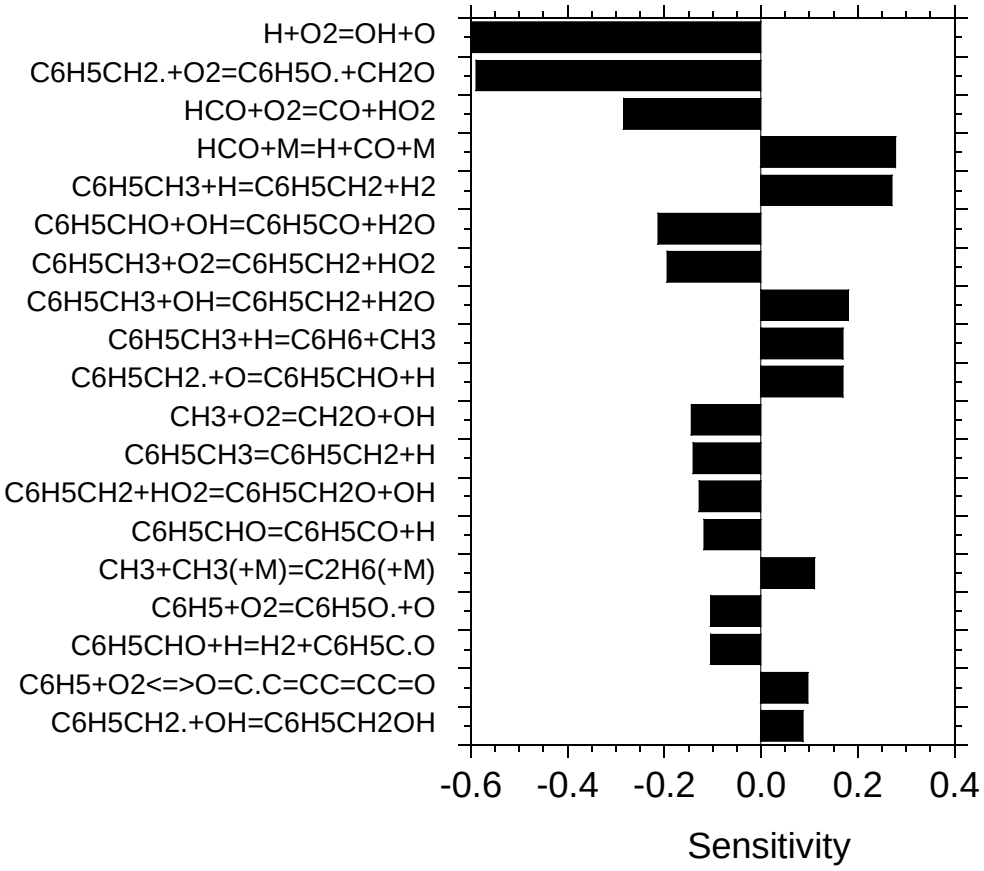

Figure 6: Sensitivity of the toluene concentration to changes in individual rate constants under flow reactor conditions. (equivalence ratio = 0.76, N_2 98 %, initial temperature = 1173 K, atmospheric pressure, residence time is 135 ms).

$$C_6H_5CH_2\cdot + O_2 = C_6H_5O\cdot + CH_2O.$$

The rate constant of this reaction, $k = 5.30\times10^{13}T^{-1.07}\exp(-10840\,\mathrm{cal}/RT)$, was taken from Zhong [4]. This reaction occurs through a 4-membered transition state where the terminal oxygen on the benzyl peroxy radical adds to the benzene ring.

The HCO + O_2 = CO + HO_2 reaction promotes fuel oxidation because it produces HO_2 radicals that react with benzyl radicals via,

$$C_6H_5CH_2\cdot + HO_2 = C_6H_5CH_2O\cdot + OH$$

a reaction with a negative sensitivity that also promotes fuel oxidation. The reaction of toluene with H atoms exhibits a positive sensitivity and retards the overall fuel oxidation rate, as seen under shock tube conditions.

Comparisons with Strained Laminar Flow under Nonpremixed Conditions

The detailed chemical-kinetic mechanism was tested by comparing computed results with experiments performed under strained, nonpremixed conditions. Numerical calculations were carried out using FlameMaster [24]. The formulation of the numerical problem is summarized elsewhere [24, 25]. At both ends of the computational domain, the mass fractions of the reactants and the normal components of the flow velocity were specified. The values of the tangential component of the flow velocity at both ends were set equal to zero (the so-called plug-flow boundary conditions). The characteristic strain rate at the stagnation plane was calculated using Eq. (1). Solutions could not be obtained with the 349 species detailed chemical-kinetic mechanism due to numerical "stiffness" problems. The detailed chemical kinetic mechanism was simplified using the NIST XSenkplot [26]. Simplified mechanisms were obtained under shock tube conditions and flow reactor conditions and combined to yield a 58 species mechanism made up of 221 reversible reactions. Any reaction in the detailed mechanism that involved only these 58 species was retained in the simplified mechanism. Ignition delay times were calculated using the simplified mechanism and the detailed mechanism at conditions similar to those employed in the shock-tube experiments. At all conditions the differences were found to be less than 14 %.

Figure 7 shows the mass fraction of toluene in the fuel stream at extinction, $Y_{\mathrm{F},1}$, as a function of the strain rate, $a_{2,e}$. The symbols represent measurements. The solid line represents results of numerical calculations performed using the simplified chemical-kinetic mechanism. At a given value of $Y_{\mathrm{F},1}$ the calculated value of $a_{2,e}$ is lower than that measured. Figure 8 shows the oxidizer temperature at autoignition, as a function of the strain rate, $a_{2,I}$. The symbols represent measurements reproduced from Refs. [11, 27]. The solid line represents results of numerical calculations performed using the simplified chemical-kinetic mechanism. At

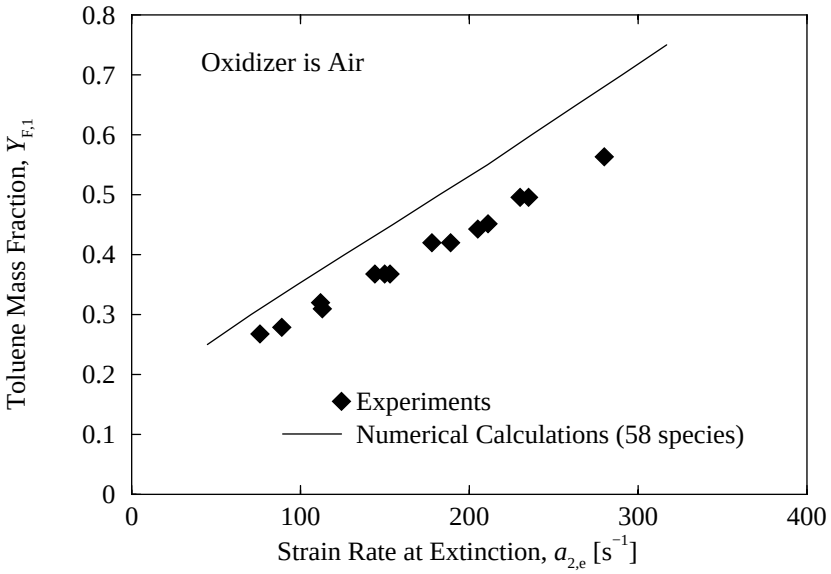

Figure 7: Mass fraction of toluene in the fuel stream at extinction, $Y_{\mathrm{F},1}$, as a function of the strain rate, $a_{2,e}$. The symbols represent measurements. The solid line represents results of numerical calculations performed using the simplified chemical-kinetic mechanism made up of 58 species.

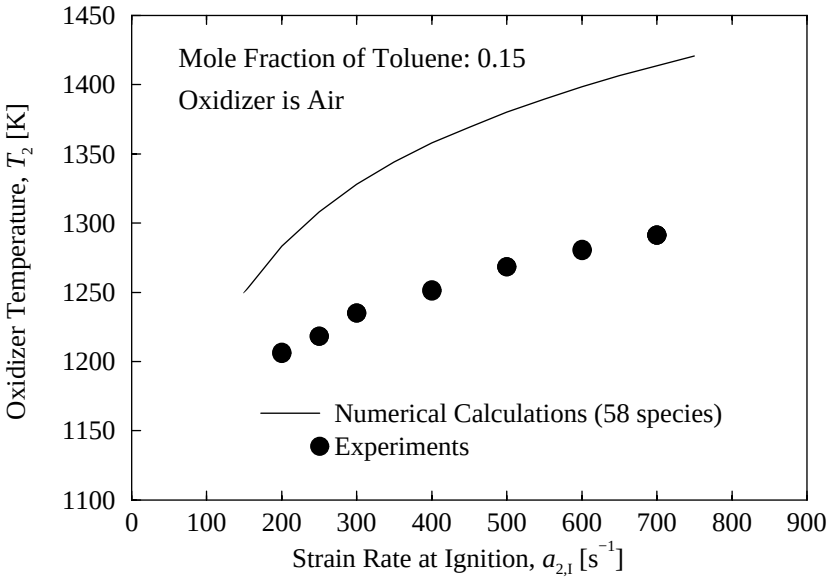

Figure 8: Oxidizer temperature at autoignition, $T_{2,I}$, as a function of the strain rate, $a_{2,I}$. The symbols represent measurements [11, 27]. The solid line represents results of numerical calculations performed using the simplified chemical-kinetic mechanism made up of 58 species.

a given value of the oxidizer temperature the calculated value of $a_{2,I}$ is lower than that measured. Thus in both extinction and ignition experiments, the numerical model predicts that toluene/air is overall less reactive than observed in the experiments. This result is consistent with comparisons between the model predictions and experimental results from the shock tube above 1400K.

The sensitivity results for autoignition under nonpremixed conditions are given in Fig. 9. The analysis performed by FlameMaster [24] gives the change in maximum OH concentration

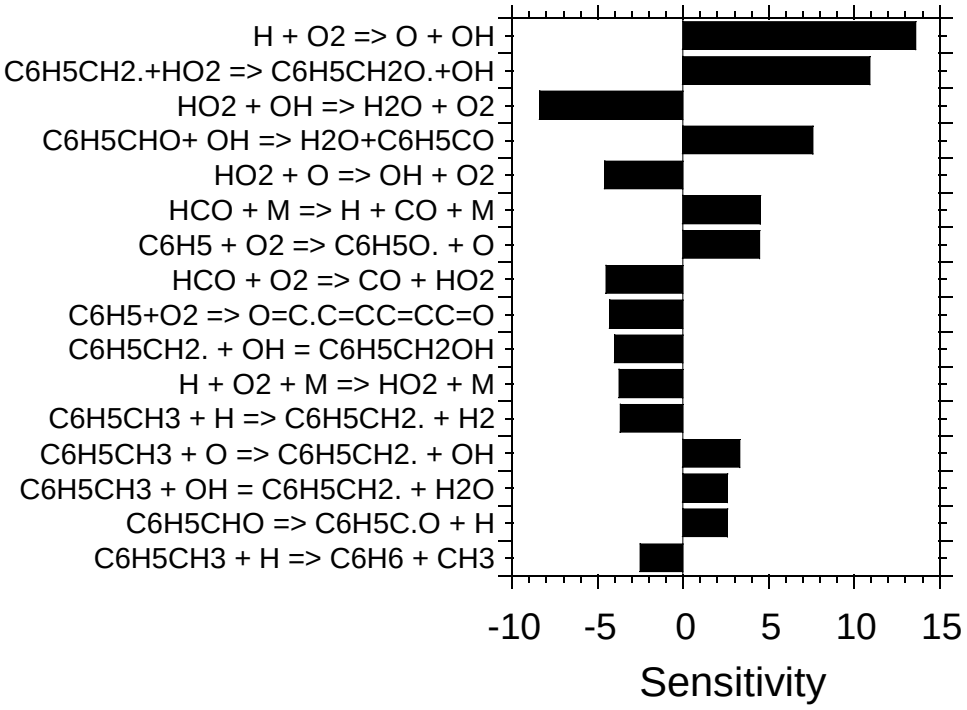

Figure 9: Sensitivity of the OH radical concentration to changes in individual rate constants under nonpremixed conditions near autoignition (strain rate = $400\,\mathrm{s}^{-1}$, oxidizer temperature $T_2 = 1357\,\mathrm{K}$).

for an incremental change in rate constant as indicated in Fig. 9. In FlameMaster, forward and reverse rate constants are considered as separate parameters for the purposes of sensitivity analysis. The analysis was performed for a reactive flow solution very near autoignition. Positive sensitivities indicate an increase in rate constant increases the OH concentration and accelerates the overall rate of reaction, while negative sensitivities indicate an increase in rate constant decreases the OH concentration and retards the overall rate of reaction. The H + O_2 chain branching reaction again gives very high sensitivity as under shock tube and flow

reactor conditions. The reaction benzyl radicals with HO_2,

$$C_6H_5CH_2\cdot + HO_2 = C_6H_5CH_2O\cdot + OH$$

exhibits a particularly high sensitivity under counterflow ignition conditions. The reaction of benzaldehyde with OH shows a high positive sensitivity and promotes ignition.

The reactions that give significant sensitivity under nonpremixed conditions but not under flow reactor or shock tube conditions are reactions that involve the phenyl + O_2 reaction:

$$C_6H_5 + O_2 \rightleftharpoons C_6H_5O\cdot + O,$$
$$C_6H_5 + O_2 \rightleftharpoons O{=}C\cdot C{=}CC{=}CC{=}O.$$

An important uncertainty in the phenyl + O_2 system is the branching ratio between the two product channels given above. The O-atom product channel is accelerating and the other ring-opening product channel is retarding (Fig. 9). The branching ratio depends on the relative barrier heights for the phenylperoxy radical going to O-O bond breakage versus to ring opening [19].

Conclusions

The detailed chemical-kinetic model for toluene was improved by adding a more accurate description of the phenyl + O_2 reactions, toluene decomposition reactions and the benzyl radical + O reaction. These reactions have been analyzed by quantum RRK to obtain $k(E)$ and by master equation for fall-off. New data obtained under nonpremixed conditions in a counterflow configuration and obtained in a shock tube were compared to results of the detailed chemical-kinetic model. Sensitivity analysis was used to identify reactions whose rate constants control the overall rate of oxidation. This information can be used to obtain future improvements of the agreement between the model and experiments. The reactions that exhibited high sensitivity (besides H + O_2 chain branching) included toluene decomposition reactions, toluene reaction with H, OH and O_2, and benzyl reaction with HO_2 and O_2. Also, phenyl + O_2 reactions were shown to be important during ignition in a nonpremixed, counterflow system. Although the benzyl + O reaction did not appear in the sensitivity analysis, it was primary reaction consuming benzyl under shock tube and flow reactor conditions.

Acknowledgments

The work at LLNL was performed under the auspices of the U.S. Department of Energy by the Lawrence Livermore National Laboratory under contract No. W-7405-ENG-48 and supported by the US Department of Energy, Office of Transportation Technologies, Steve

Chalk and Gurpreet Singh, program managers, and by the Office of Basic Energy Sciences, Division of Chemical Sciences, William Kirchhoff, program manager. The research at UCSD was supported by the Mechanical and Environmental Sciences Division of the Army Research Office through Grant #DAAD19-99-1-0259. Dr. David Mann program manager. The authors wish to thank Don Burgess for his help with XSenkplot.

References

[1] S. D. Klotz, K. Brezinsky, and I. Glassman. Modeling the combustion of tolune-butane blends. *Proceedings of the Combustion Institute*, 27:337–344, 1998.

[2] J. L. Emdee, K. Brezinsky, and I. Glassman. *Journal of Physical Chemistry*, 96:2151–2161, 1992.

[3] X. Zhong and J. W. Bozzelli. *International Journal of Chemical Kinetics*, 29:893–913, 1997.

[4] X. Zhong. Ph.D thesis, New Jersey Institute of Technology , Newark, NJ, 1998.

[5] X. Zhong and J. W. Bozzelli. *Journal of Physical Chemistry*, 102:3537, 1998.

[6] R. P. Lindstedt and L. Q. Maurice. Detailed kinetic modelling of toluene combustion. *Combustion Science and Technology*, 120:119–167, 1996.

[7] C. Venkat, K. Brezinsky, and I. Glassman. High temperature oxidation of aromatic hydrocarbons. *Proceedings of the Combustion Institute*, 19:143–152, 1982.

[8] K. Brezinsky, T. A. Litzinger, and I. Glassman. *International Journal of Chemical Kinetics*, 16:1053, 1984.

[9] J. F. Griffiths, P. A. Halford-Maw, and D. J. Rose. Fundamental features of hydrocarbon autoignition in a rapid compression machine. *Combustion and Flame*, 95:291–306, 1993.

[10] A. Roubaud, R. Minetti, and L. R. Sochet. Oxidation and combustion of low alkylbenzenes at high pressures: Comparitive reactivity and auto-ignition. *Combustion and Flame*, 121:535–541, 2000.

[11] R. Seiser, K. Seshadri, E. Piskernik, and A. Liñán. Ignition in the viscous layer between counterflowing streams: Asymptotic theory with comparison to experiments. *Combustion and Flame*, 122:339–349, 2000.

[12] E. L. Peterson, D. F. Davidson, and R. K. Hanson. *Journal of Propulsion and Power*, 15:591–600, 1999.

[13] K. Seshadri and F. A. Williams. Laminar flow between parallel plates with injection of a reactant at high Reynolds number. *International Journal of Heat and Mass Transfer*, 21(2):251–253, 1978.

[14] R. Seiser, L. Truett, D. Trees, and K. Seshadri. Structure and extinction of non-premixed n-heptane flames. *Proceedings of the Combustion Institute*, 27:649–657, 1998.

[15] H. J. Curran, P. Gaffuri, W. J. Pitz, and C. K. Westbrook. A comprehensive modeling study of n-heptane oxidation. *Combustion and Flame*, 114:149–177, 1998.

[16] R. Seiser, H. Pitsch, K. Seshadri, W. J. Pitz, and H. J. Curran. Extinction and autoignition of n-heptane in counterflow configuration. *Proceedings of the Combustion Institute*, 28:2029–2037, 2000.

[17] Chemical-kinetic mechanism for toluene. http://www.llnl.gov/combustion/combustion-home.html, 2001.

[18] H. J. Curran, W. J. Pitz, C. K. Westbrook, C. V. Callahan, and F. L. Dryer. Oxidation of automotive primary reference fuels at elevated pressures. *Proceedings of the Combustion Institute*, 27:379–387, 1998.

[19] J. Bozzelli, N. Sebbar, W. Pitz, and H. Bockhorn. Reaction of phenyl radical with O_2: Thermodynamic properties, important reaction paths and kinetics. In *Paper #99, 2nd Joint Meeting of the US Sections of the Combustion Institute*, Oakland, California, March 21-28 2001.

[20] C. J. Chen and J. W. Bozzelli. *Journal of Chemical Physics*, 104:9715–9732, 2000.

[21] R. W. Walker. Kinetics and mechanism of hydrocarbon oxidation in the middle temperature regime. In *Joint Meeting of the British, German and French Sections of the Combustion institute*, May 1999.

[22] R. J. Kee, F. M. Rupley, J. A. Miller, M. E. Coltrin, J. F. Grcar, E. Meeks, H. K. Moffat, A. E. Lutz, G. Dixon-Lewis, M. D. Smooke, J. Warnatz, G. H. Evans, R. S. Larson, R. E. Mitchell, L. R. Petzold, W. C. Reynolds, M. Caracotsios, W. E. Stewart, P. Glarborg, C. Wang, and O. Adigun. CHEMKIN collection, release 3.6. Reaction Design, Inc., San Diego, California, 2000.

[23] D. L. Baulch, C. J. Cobos, R. A. Cox, C. Esser, P. Frank, Th. Just, J. A. Kerr, M. J. Pilling, J. Troe, R. W. Walker, and J. Warnatz. *Journal of Physical and Chemical Reference Data*, 21:411–429, 1992.

[24] H. Pitsch. Entwicklung eines Programmpaketes zur Berechnung eindimensionaler Flammen am Beispiel einer Gegenstromdiffusionsflamme. Master's thesis, RWTH Aachen, Germany, 1993.

[25] N. Peters. Flame calculations with reduced mechanisms - an outline. In N. Peters and B. Rogg, editors, *Reduced Kinetic Mechanisms for Applications in Combustion Systems*, volume m15 of *Lecture Notes in Physics*, chapter 1, pages 1–13. Springer-Verlag, Heidelberg, 1993.

[26] D. R. Burgess. NIST XSenkplot: An interactive, graphics postprocessor for numerical simulations of chemical kinetics. http://www.cstl.nist.gov/div836/xsenkplot, Reacting Flow Group, Process Measurements Division, Chemical Science and Technology Laboratory, National Institute of Standards and Technology, 1996.

[27] R. Seiser, H. Pitsch, K. Seshadri, H. J. Curran, and W. J. Pitz. Experimental and numerical studies of extinction and autoignition of n-heptane. paper presented at the Fall Meeting of the Western States Section of the Combustion Institute, The University of California at Irvine, Irvine, California, October 25, 26, 1999.

Appendix B: The Structure of Nonpremixed *n*-Decane Flames

K. Tanoue, R. Seiser, K. Seshadri

Abstract

Experiments are conducted on flames stabilized between two counterflowing streams. The fuel stream is a mixture of prevaporized *n*-decane and nitrogen, and the oxidizer stream is a mixture of air and nitrogen. Concentration profiles of $C_{10}H_{22}$, O_2, N_2, CO_2, CO, H_2O, CO, CH_4, and hydrocarbons ranging from C_2 up to C_9, are measured. The measurements are made by removing gas samples from the flame using a quartz microprobe and analyzing the samples using a gas chromatograph. Temperature profiles are measured using a thermocouple. Critical conditions of extinction and critical conditions of autoignition are measured. Numerical calculations are performed using detailed chemistry to determine the flame structure and to obtain values for extinction and autoignition.

Introduction

The combustion of *n*-decane has been studied experimentally by various investigators. Previous studies were conducted on shock-tubes [1], jet-stirred-reactors [2], flow-reactors [3], burner stabilized [4, 5], and freely propagating premixed flames [6]. The present experimental investigation reports experimental data obtained for a nonpremixed *n*-decane flame in a counterflow configuration. In the following, the experimental method is described, and data for stable species and temperature are reported. In addition, data for extinction and autoignition are provided.

Description of Experimental and Numerical Studies

Studies are conducted on nonpremixed *n*-decane flames stabilized in the counterflow configuration. For temperature and species profiles the fuel stream contains *n*-decane with a mole fraction of $X_{C_{10}H_{22}}$=0.08 and nitrogen. The oxidizer stream is air. The strain rate a_2=100 s^{-1} and is calculated by the formula [7]

$$a_2 = \frac{2|V_2|}{L}\left(1 + \frac{|V_1|\sqrt{\rho_1}}{|V_2|\sqrt{\rho_2}}\right). \tag{1}$$

Here, V denotes the velocity and ρ the density. Subscripts 1 and 2 refer to the fuel stream and oxidizer stream, respectively. The separation distance between the two ducts is L=10 mm. The momenta of the two opposing streams are balanced as described by $\rho_1 V_1^2 = \rho_2 V_2^2$. Plug-flow conditions are assumed. Details and dimensions of the counterflow burner are given in Refs. [8] and [9]. Figure 1 shows the setup for temperature and species profile measurements. Concentrations of stable species are measured by removing gas samples from the reaction zone using a quartz microprobe and analyzing them in a gas chromatograph. The microprobe has a tip with an outer diameter of 166 microns and an inner diameter of 83 microns. The tip is placed at a location of 5 mm off the centerline of the ducts to avoid disturbance of

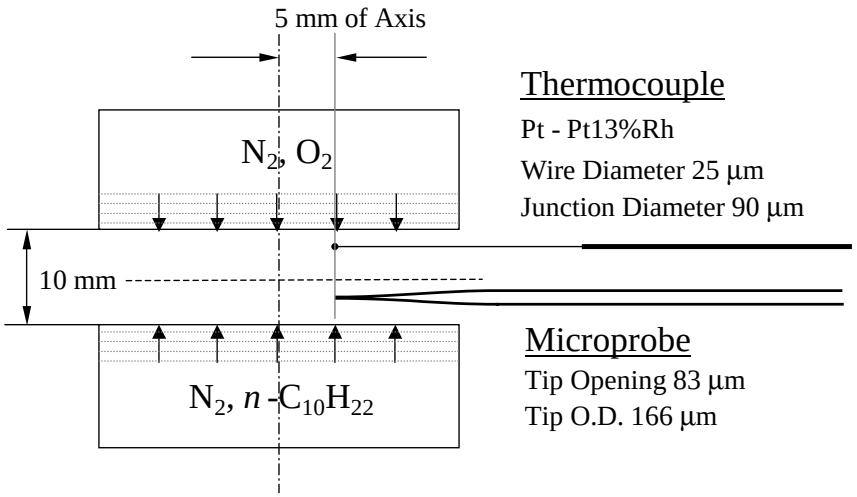

Figure 1: Temperature and species profile measurements in a nonpremixed *n*-decane flame.

the flow-field and influencing the reactive diffusive balance in the vicinity of the probe. The species concentrations and temperatures are assumed to be only functions of the coordinate along the centerline [10]. The samples drawn from the flame are quantified using a SRI 8610C gas chromatograph. The instrument is equipped with with a 4.5ft mole-sieve (80/100 mesh) - for separating H_2, O_2 and Ar, N_2, CH_4, and CO - and a 12ft Porapaq Q column for separating all other species. Temperature programming and valve switching is employed to optimize the separation performance of both columns. The species eluding from the column are quantified using a thermo-conductivity-detector (TCD) and a flame-ionization-detector (FID). The chromatograms are analyzed using self written software, and by comparing with runs of known samples, the absolute mole fractions are determined. For species where no calibration gases were used, we determined the calibration factors by inter- or extra-polating around known species. This was done by plotting the FID-calibration factors as a function of the number of C-atoms. In one curve for the paraffins, species measured comprise ethane, propane, *n*-heptane, *n*-octane, and *n*-decane. A second curve for the alkenes was similarly established by calibrating ethene, propene, 1-butene, and 1-hexene. All species of C_4-hydrocarbons are reported as one concentration, because individual separation and calibration was not possible. Similarly C_5-, C_6-, C_7-, C_8-, and C_9-hydrocarbons are reported, here assuming that they are mostly comprised by 1-alkenes, and thus using the 1-alkene calibrations. Ethene and ethyne appeared as single peak and are reported as their sum using the calibration for ethene. Previous analysis using a mass-spectrometer has shown that for a *n*-heptane flame the amount of ethene is slightly larger than that of ethyne [11]. Argon eluded together with oxygen from the columns. By assuming the Lewis number of argon and the Lewis numbers of the main species to be equal, the amount of argon at any point in the flow-field was determined from the mixture-fraction (calculated using the carbon mass fraction from the measured species) and the amount of argon in the oxidizer stream (Y_{Ar}=0.01313). Water appeared as peak

with a long tail on the TCD-detector. The area of this peak was determined by using a linear baseline starting at the onset of the water signal and parallel to the baseline for a measurement containing no water. By choosing a proper balance of pressure and temperature of the sampling probe, sampling line, and sample loop, we were able to measure all water without experiencing condensation. This, however, was not possible for certain measurements containing *n*-decane, as its boiling point is much higher than that of water. We therefore only report values of *n*-decane smaller than $X_{C_{10}H_{22}}$=0.03. Closer to the fuel-side, the amounts of *n*-decane are estimated using a numerical calculation of a Burke-Schumann (subscript BS) solution. In these locations the amounts of all other species can then be determined by using the measured values and normalizing them so that their sum equals (1.0 - $X_{C_{10}H_{22},BS}$). The expected accuracy for the maximum concentrations of most species is expected to be better than ±10%. This includes species that can be clearly identified on either the FID or TCD-detector. Hydrogen gives a very small signal on the TCD-detector and it is estimated to be accurate to ±25%. The expected accuracy for water is asumed to be ±20%. At this point the accuracy for C_7-C_9 species is not quantifiable, as their absolute concentrations are small and possibly influenced by radical recombination in the probe. The temperature profile was measured using an uncoated Pt-Pt13%Rh (Type R) thermocouple. The wire diameter is 25 microns and the bead diameter is 90 microns. The measurement is corrected for radiation by assuming spherical shape of the bead and a constant emissivity of 0.2. Catalytic effects are neglected. The absolute accuracy of the temperature measurement is expected to be better than ±80 K. The location of the sampling probe and the thermocouple in the flow-field is determined using a digital photo camera. The size of one pixel corresponds to a distance in the flow-field of approximately 17 microns.

Extinction measurements are performed for various *n*-decane concentrations in the fuel stream. The oxidizer stream is air. For a certain composition of the reactant streams, a flame is established, and the the strain rate is increased until extinction is observed. The autoignition experiments are performed for a mole fraction of *n*-decane $X_{C_{10}H_{22}}$=0.15. The oxidizer stream is air, and it is heated until autoignition is observed. In the extinction and ignition experiments the separation distance of the ducts is 10 mm and 12 mm, respectively. The temperature of the fuel stream is 400 K in the extinction experiments, and 408 K in the ignition experiments.

Numerical calculations are performed using detailed chemistry, applying the same boundary conditions as in the experiments. For the computations the computer program FlameMaster is used, which was developed at RWTH-Aachen [12]. The conservation equations of mass, momentum and energy and the species balance equations used in the formulation of the numerical problem are summarized elsewhere [12–14]. The species balance equations include thermal diffusion and the energy conservation equation includes radiative heat losses from carbon dioxide and water vapor [12]. Plug-flow boundary conditions are used. Buoyancy is neglected. As chemical-kinetic mechanism, a detailed mechanism by Bikas et al. [15] containing 347 reversible reactions among 66 species, is used.

Results and Discussion

Figure 2 shows experimental data on the temperature field in the nonpremixed n-decane flame.

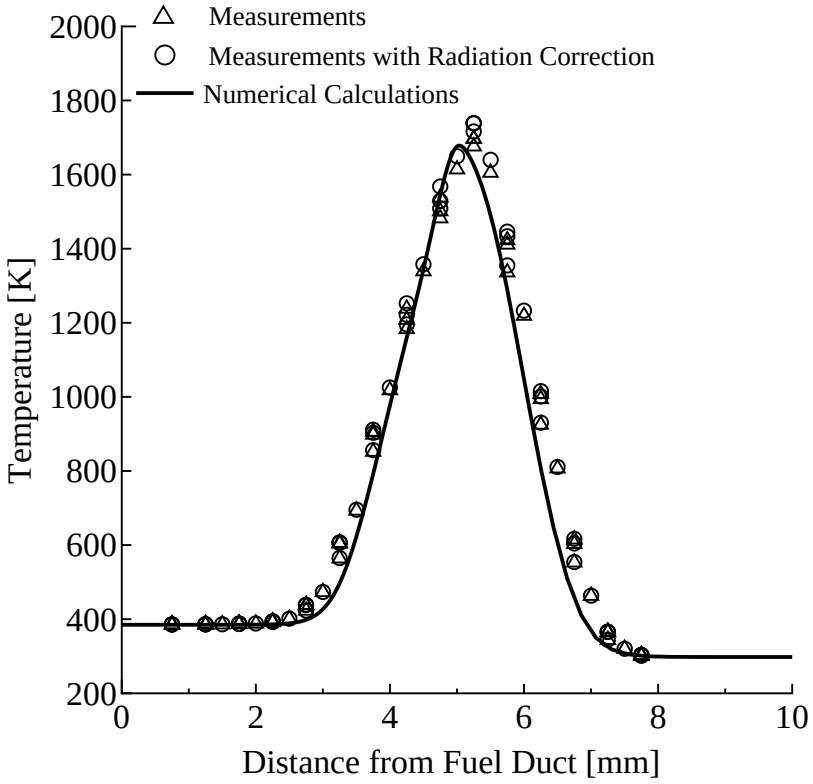

Figure 2: Temperature measurement in a nonpremixed n-decane flame. The triangles represent the raw-data of the measured temperature, the spheres represent the temperature corrected for radiation. The lines are results of numerical calculations using detailed chemistry.

The triangles show the temperature of the thermocouple as read from the temperature display unit. After a radiation correction is applied, that takes into account the radiation from the surface of the thermocouple, the gas temperature is obtained, shown as spheres in Fig. 2. The corrected temperature agrees well with the computed one, concerning the maximum temperature, shift and broadness of the temperature profile. Figure 3 shows experimental data on the main species in the n-decane flame. The agreement between measured and calculated concentrations is very good. CO_2, H_2O, and CO are the main products of combustion and are usually well predicted by chemical-kinetic mechanisms. The comparison in Fig. 3 is therefore an indication of the flow-field and the influence by the microprobe. The influence of the microprobe on the reactive-diffusive balance is usually high closer to the ducts where the axial velocity – perpendicular to the probe – is higher. In the reaction zone, heat loss to the probe can cause local quenching and cause stronger oxygen leakage. From the profile for oxygen it can be seen that the measured leakage is slightly higher than predicted by the numerical calculation. The chemical-kinetic mechanism, however, predicts a higher extinction strain

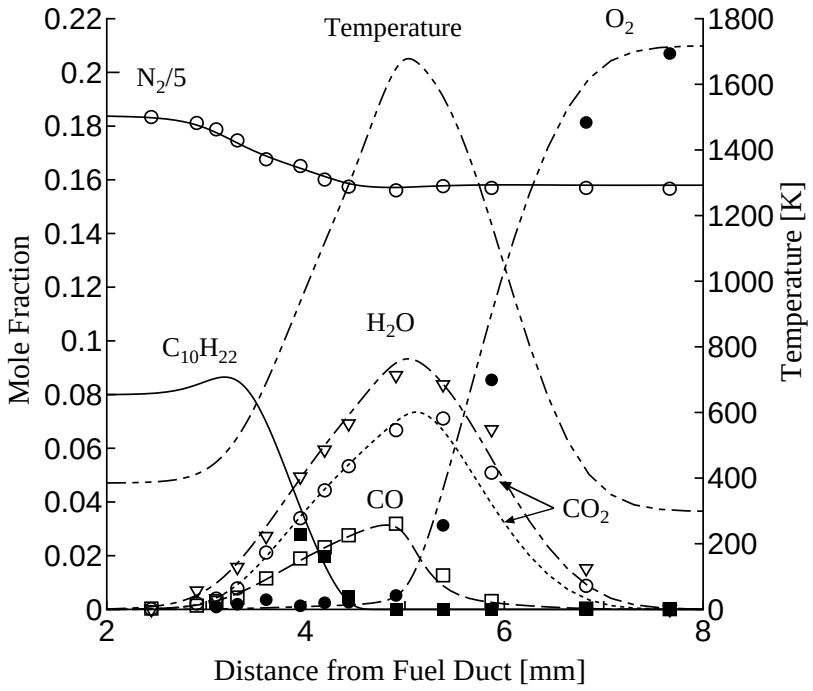

Figure 3: Experimental data showing the mole fraction of $C_{10}H_{22}$, O_2, CO_2, H_2O, and CO as a function of distance. The points represent measurements and the lines are results of numerical calculations using the chemical-kinetic mechanism by Bikas et al. [15].

rate, and therefore less leakage at the measured strain rate of $100\,s^{-1}$. The influence of the microprobe can therefore be assumed to be minimal. Figures 4 and 5 show experimental data on intermediate species of small molecular weight. The profiles of C_2H_2+C_2H_4, H_2, and C_3H_8 agree well with numerical calculations. The chemical-kinetic mechanism under-predicts CH_4, C_2H_6, and C_3H_6 by about 30-70%. Figures 6 and 7 show experimental data on concentrations of larger stable hydrocarbon species. Radical species are usually small and will recombine in the sampling probe to form stable species. The numerical computations for C_4-species somewhat over-predict measured concentrations, while computations of stable C_5- and C_6-species are lower than the experimental data. Measured stable C_7-hydrocarbons are much larger than predicted. The calculated values for the sum of all C_7-species (including radical species) are everywhere below a mole fraction of 10^{-8}. For C_8- and C_9-species, no stable species appeared in the chemical-kinetic mechanism. Figure 8 shows experimental data on extinction of a nonpremixed *n*-decane flame with variable fuel concentrations. The results are compared with numercal calculations using the chemical-kinetic mechanism of Bikas et al. [15]. The mechanism agrees reasonably well with experiments. Figure 9 shows experimental data on autoignition of a nonpremixed *n*-decane / air system. The numerical calculations agree well with experiments, especially at lower strain rates. At higher strain rates the mechanism predicts slightly lower autoignition temperatures.

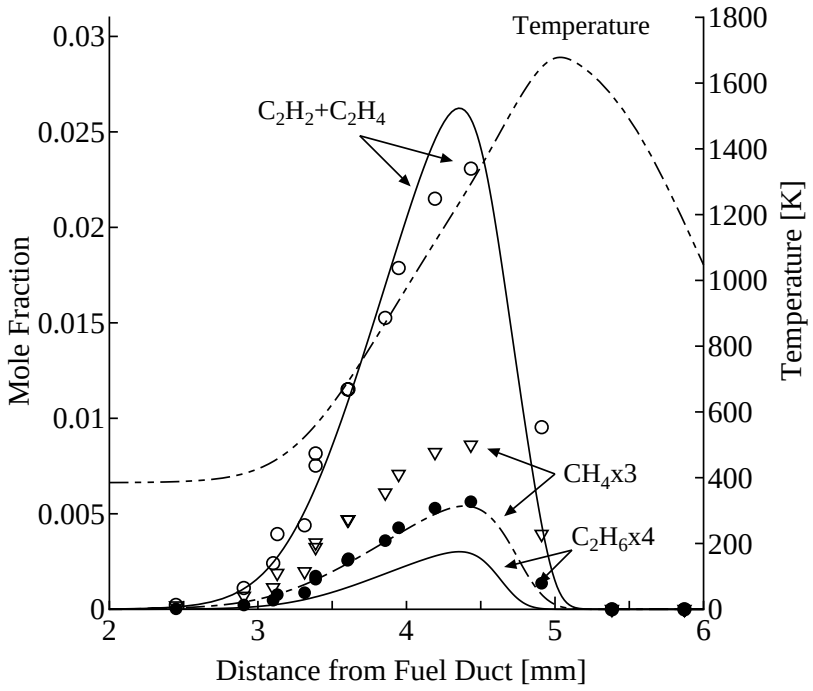

Figure 4: Experimental data showing the mole fraction of C_2H_2+C_2H_4, CH_4, and C_2H_6 as a function of distance. The points represent measurements and the lines are results of numerical calculations.

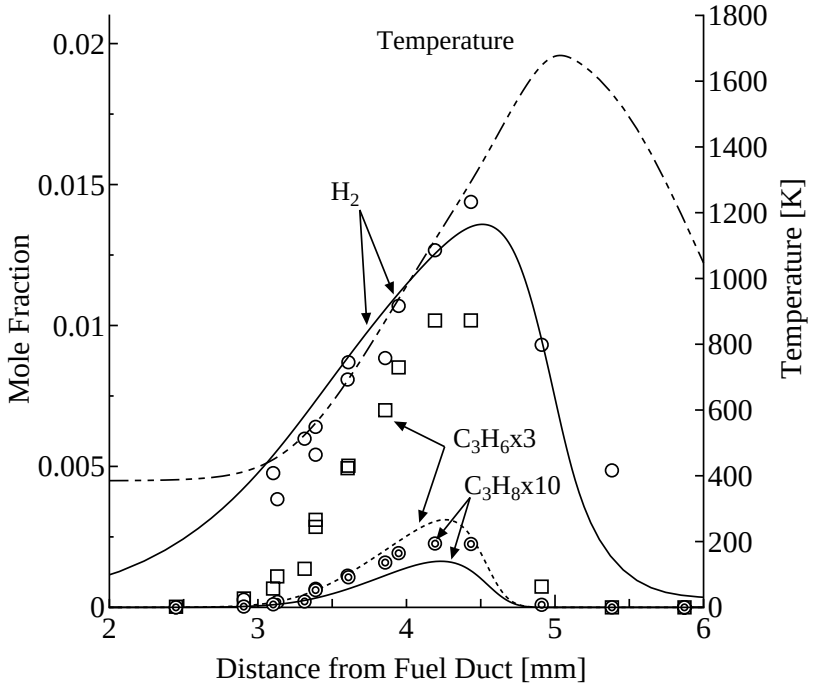

Figure 5: Experimental data showing the mole fraction of H_2, C_3H_6, and C_3H_8 as a function of distance. The points represent measurements and the lines are results of numerical calculations.

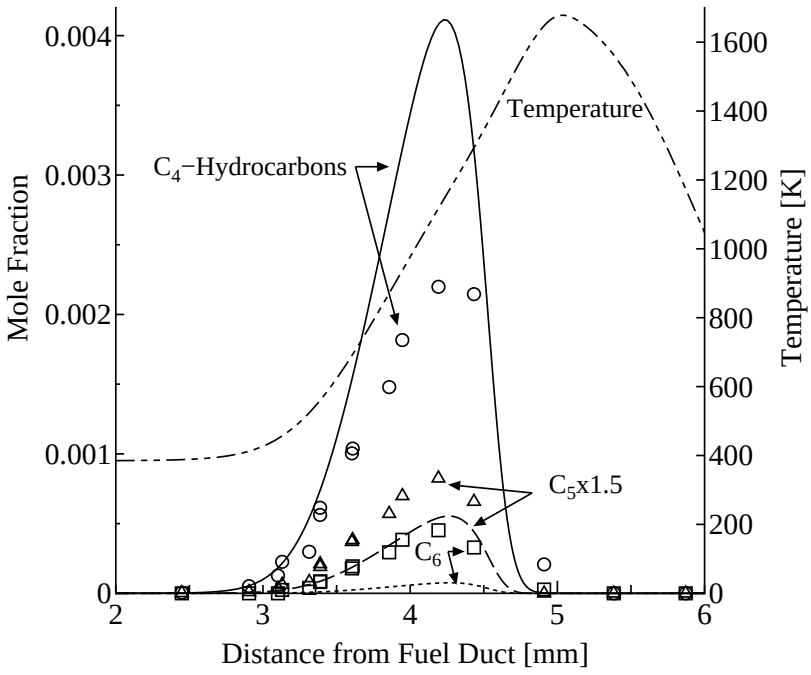

Figure 6: Experimental data showing the mole fraction of C_4-, C_5-, and C_6-hydrocarbons as a function of distance. The points represent measurements and the lines are results of numerical calculations. The numerically computed temperature is shown for reference.

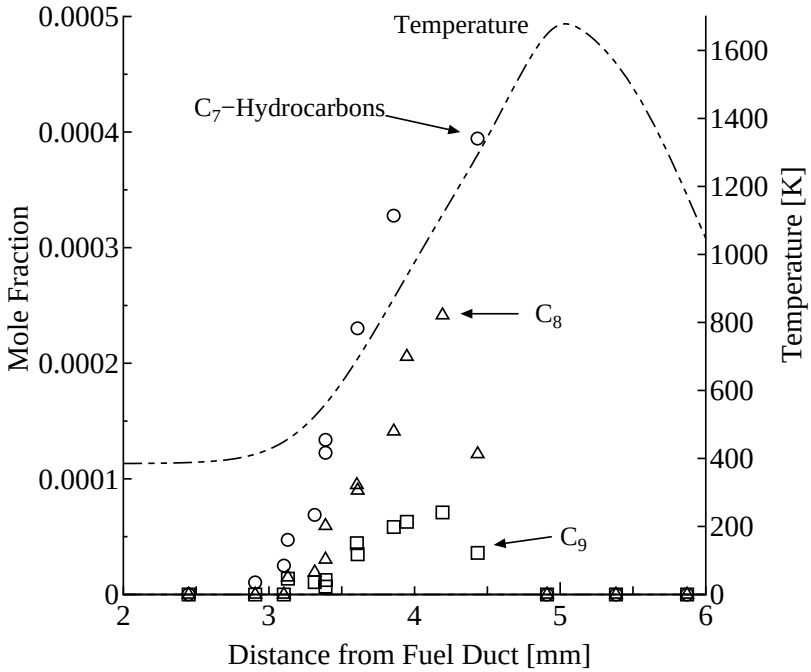

Figure 7: Experimental data showing the mole fraction of C_7-, C_8-, and C_9-hydrocarbons as a function of distance. The points represent measurements. The numerically computed temperature is shown for reference.

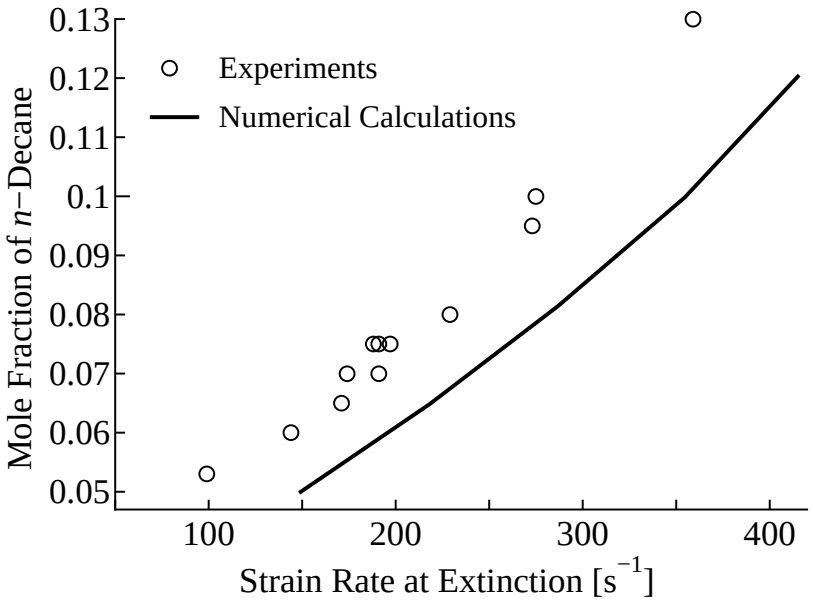

Figure 8: Extinction of nonpremixed *n*-decane flame. The mole fraction of *n*-decane in the fuel stream is plotted versus the strain rate. The oxidizer stream is air. The temperatures of the fuel stream and oxidizer stream are 400 K and 298 K. The symbols represent measurements and the lines are results of numerical calculations.

References

[1] Pfahl U., Fieweger K., and Adomeit G., *Proceedings of the Combustion Institute* 26:781–789 (1996).

[2] Balès-Guéret C., Cathonnet M., Boettner J.C., and Gaillard F., *Energy Fuels* 6:189–194 (1992).

[3] Zeppieri S.P., Klotz S.D., and Dryer F.L., *Proceedings of the Combustion Institute* 28:1587–1595 (2000).

[4] Douté C., Delfau J.L., Akrich R., and Vovelle C., *Combustion Science and Technology* 106:327–344 (1995).

[5] Delfau J.L., Bouhria M., Reuillon M., Sanogo O., Akrich R., and Vovelle C., *Proceedings of the Combustion Institute* 23:1567–1572 (1990).

[6] Wagner P. and Dugger G.L., *Journal of American Chemical Society* 77:227 – 231 (1955).

[7] Seshadri K. and Williams F.A., *International Journal of Heat and Mass Transfer* 21, 2:251–253 (1978).

[8] Seiser R., *Nonpremixed combustion of liquid hydrocarbon fuels*, Ph.D thesis, Technical University of Graz, 2000.

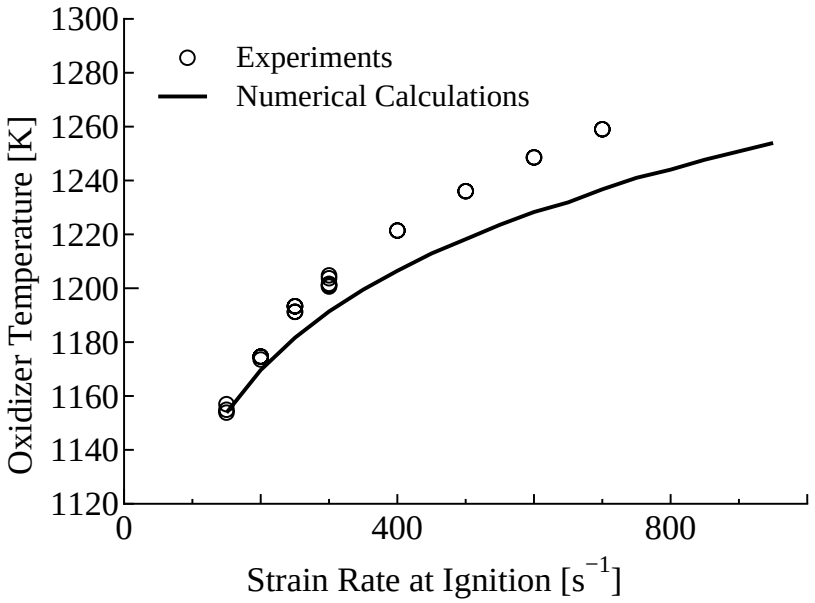

Figure 9: Autoignition of a nonpremixed *n*-decane flame. The oxidizer temperature at autoignition is plotted versus the strain rate. The mole fraction of *n*-decane is 0.15. Oxidizer is air. The symbols represent measurements and the lines are results of numerical calculations.

[9] Humer S., Seiser R., and Seshadri K., *Proceedings of the Combustion Institute* 29:0 (2002), in press.

[10] Fendell F.E., *Journal of Fluid Mechanics* 21, 2:281–303 (1965).

[11] Seiser R., Truett L., Trees D., and Seshadri K., *Proceedings of the Combustion Institute* 27:649–657 (1998).

[12] Pitsch H., *Entwicklung eines Programmpaketes zur Berechnung eindimensionaler Flammen am Beispiel einer Gegenstromdiffusionsflamme*, Master's thesis, RWTH Aachen, Germany, 1993.

[13] Peters N., Peters N. and Rogg B. (eds.), *Reduced Kinetic Mechanisms for Applications in Combustion Systems*, vol. m15 of *Lecture Notes in Physics*, Springer-Verlag, Heidelberg, 1993, chap. 1, pp. 1–13.

[14] Bollig M., Pitsch H., Hewson J.C., and Seshadri K., *Proceedings of the Combustion Institute* 26:729–737 (1996).

[15] Bikas G. and Peters N., *Combustion and Flame* 126:1456–1475 (2001).

Appendix C: Autoignition and Extinction of Hydrocarbon Fuels in Nonpremixed Systems

S. Humer, R. Seiser, K. Seshadri

Abstract

Experimental studies are carried out on extinction and autoignition of liquid hydrocarbon fuels in nonpremixed systems. The counterflow configuration is employed in the experimental studies. In this configuration an oxidizer made up of air and nitrogen flows over the surface of a pool of liquid fuel. Critical conditions of extinction and autoignition are measured for *n*-heptane, iso-octane, *n*-octane, *n*-decane, *n*-dodecane, *n*-hexadecane, o-xylene, JP-10, diesel, and JP-8.

Introduction

Fundamental studies on extinction and autoignition of strained flames provide knowledge for modeling turbulent combustion. Previous studies on autoignition of reactant mixtures were focused on measuring ignition delay time in shock tubes [1] and rapid compression machines [2]. These studies do not characterize the influence of strain on autoignition. In this study the influence of strain on the critical conditions of extinction and autoignition of flames is investigated.

Increasingly diesel is the fuel of choice in the automobile industry in Europe in view of fuel economy and higher efficiency of diesel engines compared to gasoline engines. Up to 70 % of the new registered cars are equipped with diesel engines. The high complexity of higher hydrocarbon fuels makes it useful to develop a model fuel of chemical characteristics similar to that of diesel to keep calculation efforts low. These model fuels can be used in test engines as well as in numerical simulations of engine performance and rates of pollutant formation. The study should provide information about fuels to be used as a base for a diesel model fuel.

The researched fuels were investigated in a simple geometry, a laminar flame in a counterflow configuration. A previous research was conducted in a similar configuration by R. Seiser et al. [3]. Although diesel engines burn the fuel in turbulent spray combustion at high pressure, the flame on the surface of a tiny droplet can be considered as a laminar non-premixed flame [4].

Description of Experimental Setup

The counterflow configuration is employed in the experimental studies. Figure 1 shows a schematic illustration of the counterflow configuration. In this design a duct is mounted above a liquid pool. The oxidizer stream is injected from this upper duct called the oxidizer duct. The oxidizer stream, made up of air and nitrogen, flows over the surface of a pool of liquid fuel at atmospheric pressure. Concentric ducts surround the oxidizer duct and the cup of the liquid pool. This outer duct provides a curtain flow of nitrogen, N_2, surrounding the inner flow. This curtain stream of N_2 shields the inner flow, containing the reactants, from influences of the surrounding. A stagnation plane is formed and the exhaust products are drawn into the exhaust system (not shown).

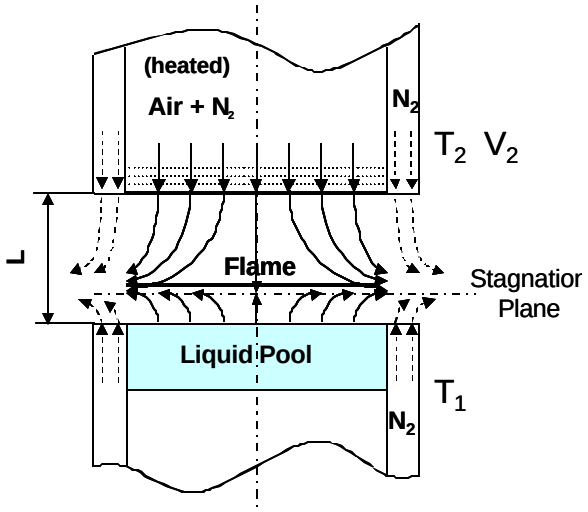

Figure 1 Schematic illustration of the liquid pool configuration.

In the exhaust system the exhaust gases get cooled down by water sprays to prevent the unburned reactants from ignition. To achieve a uniform velocity profile at the end of the oxidizer duct, three layers of a fine screen of 200 mesh are mounted at the duct exit.

The distance between the surface of the liquid pool and the exit of the oxidizer duct is L. At the exit of the oxidizer duct, the value of the injected velocity is V_2, the temperature T_2, the density ρ_2, and the mass fraction of oxygen $Y_{O2,2}$. The subscript 2 represents conditions at the exit of the oxidizer duct. At the surface of the liquid pool the temperature T_1 can be obtained from the equations describing the vapor-liquid equilibrium. For simplicity, T_1 is presumed to be equal to the normal boiling point.

The strain rate characterizing the flow field is given by

$$\mathbf{a} = \frac{2|\mathbf{V}_2|}{\mathbf{L}} \qquad \textbf{(1)}$$

This equation is obtained from an asymptotic theory where the Reynolds number of the laminar flow at the boundary is presumed to be large [5].

Critical conditions of extinction are given by the strain rate a_E and the oxygen mass fraction. Critical conditions of autoignition are given by the strain rate a_I and the temperature at the oxidizer boundary $T_{2,I}$. The extinction experiments are carried out at room temperature. The fuels tested are *n*-heptane, iso-octane, *n*-octane, *n*-decane, *n*-dodecane, *n*-hexadecane, o-xylene, JP-10, diesel, and JP-8.

Experimental Procedure

A detailed description of the burner employed in the experiments is given elsewhere [6]. Computer-regulated flow controllers measure the flow rates of the gases. The calibrated accuracy of these mass flow controllers is ±1%. The velocities of the reactants at the boundaries are presumed to be equal to the ratio of their volumetric flow rates to the cross-section area of the duct. The temperature of the oxidizer stream is measured by a thermocouple at the exit of the duct. The measured temperature is corrected for radiation by the equation $T_g = T_{tc}+(\varepsilon\cdot\sigma\cdot d\cdot T_{tc}^4/2\lambda)\cdot A$ where T_g is the gas temperature and T_{tc} is the thermocouple temperature, σ the Boltzman constant ($5.67\cdot10^{-8} W/m^2K^4$), λ the thermal conductivity, d the bead diameter of the thermocouple, and A the view factor.

Extinction Experiments

In extinction experiments the distance between the oxidizer duct and the liquid pool is L = 10 mm. The temperature of the oxidizer stream at the boundary was maintained at a constant value of 298 K. At given values of oxygen mass fraction and a strain rate the flame is stabilized in the mixing layer between the oxidizer duct and the surface of the pool. The velocity of the oxidizer stream is increased until the flame extinguishes.

Autoignition Experiments

In the autoignition experiments the distance between the duct and the liquid pool is L = 12 mm. The oxidizer mole fraction is held constant at $X_{O2,2}$ = 0.21 (mass fraction $Y_{O2,2}$ = 0.233). The oxidizer and the evaporating fuel are mixing continuously close above of the stagnation plane (see Figure 1). At a certain strain rate the oxidizer temperature is gradually increased until autoignition takes place.

Results and Discussion

Extinction

Figure 2 shows the experimental data as a function of the oxygen mass fraction $Y_{O2,2}$ over the strain rate a_E at extinction in.

For a given fuel type and oxygen mass fraction, the flame will extinguish if the strain rate of the oxidizer is higher than $a_{2,E}$. That means that for a given value of oxygen mass fraction the region $a_2<a_E$ represents an area of flammable conditions.

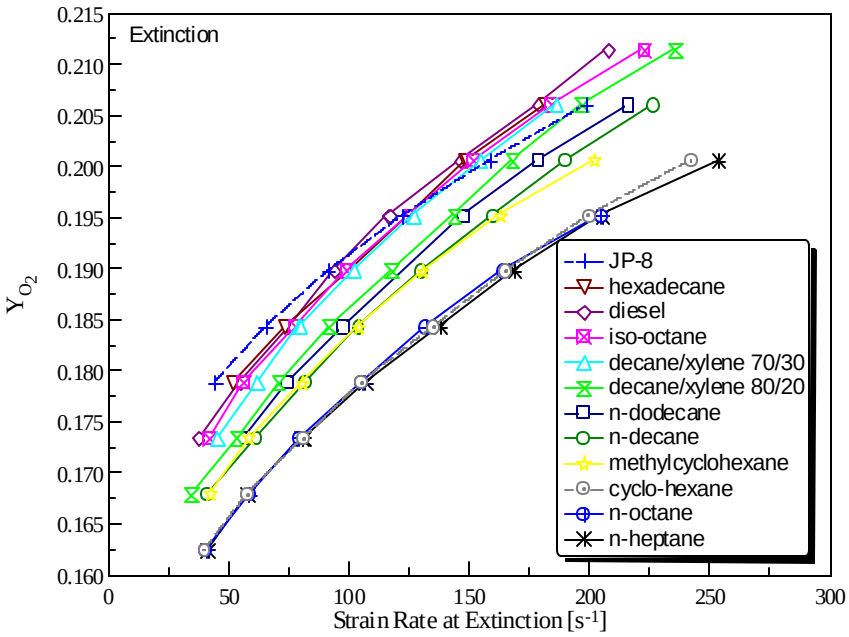

Figure 2 Experimental data showing the oxygen mass fraction $Y_{O2,2}$ as a function of the strain rate a_E at extinction. The symbols represent measurement.

All studied fuels show the same tendency. The strain rate at extinction increases with increase of the oxygen mass fraction. Also, the investigated fuels show a degressive behavior. With increasing strain rate the mass fraction $Y_{O2,2}$ also increases, but the higher the strain rate, the smaller the oxygen mass fraction difference between two adjacent measurement point.

The order of the reactivity of different fuels is nearly independent from the strain rate. Fuels with a smaller value of C-atoms are generally more reactive then fuels with long-chained carbons. Not surprisingly is that adding a less reactive fuel to another fuel decreases the overall reactivity of fuel mixture as it is done in this study for *n*-decane mixing with o-xylene. With certain combinations it is possible to achieve a fuel mixture that shows similarly chemical characteristics as e.g. diesel. That doesn't imply that a found mixture with the desired behaviors for extinction shows the same behavior for ignition.

Autoignition

Figure 3 shows the experimental data of the oxidizer temperature $T_{2,I}$ as a function of the strain rate a_2 at autoignition. These data represent the critical conditions of autoignition of liquid fuels. The symbols indicate measurements.

At a given value of strain rate, autoignition will take place if the temperature of the oxidizer stream is greater than $T_{2,I}$.

Experimental data show that the value of $T_{2,I}$ increases with increasing a_2. The fuel with the highest autoignition temperature is o-xylene followed by iso-octane. The lowest oxidizer temperature for autoignition is necessary for hexadecane. That means that hexadecane is easier to ignite than o-xylene and applies also for the order of the fuels in between. Noteworthy is the crossover between *n*-decane and *n*-dodecane among the other tested fuels. *n*-Decane and *n*-dodecane ignite easier at lower strain rate than at higher strain rate compared to the other fuel types. Also diesel and *n*-octane show a faster decrease in reactivity over the strain rate compared to the other investigated fuels. That means that there is an influence of the strain rate.

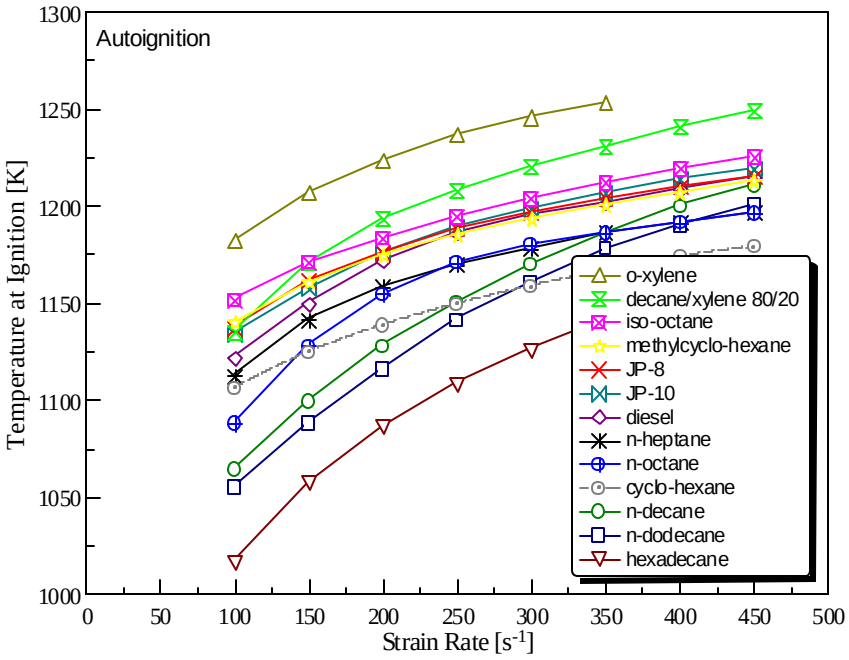

Figure 3 Experimental data showing the oxidizer temperature $T_{2,I}$ as a function of the strain rate a_2 at autoignition. The symbols represent measurements.

Conclusion

Model fuels that show similar chemical behaviors as diesel can be developed by mixing higher and lower reactive short-chained fuels.

Previous studies considered *n*-heptane as surrogate diesel. The present study shows that *n*-heptane does not reproduce extinction and autoignition characteristics of diesel. A mixture consisting of *n*-decane and o-xylene is a quite good approach to create a model fuel for diesel. In both experiments the mixture of *n*-decane 80% and o-xylene 20% shows slightly too high values compared to the results of diesel.

References

1. Ciezki, H. K., and Adomeit, G., *Combustion and Flame*, 93:421-433 (1993)

2. Minetti, R., Carlier, M., Ribaucour, M., Therssen, E., and Sochet, L. R., *Combustion and Flame*, 102:298-309 (1995)

3. Seiser, R, Seshadri, K., Chemical Kinetic Characterization of Model Fuels Used for Describing Combustion of Diesel, Diesel Engine Emissions Reduction. (1997)

4. Peters, N., Laminar diffusion flamelet models in non-premixed turbulent combustion. Institute für Allgemeine Mechanik, RWTH Aachen, Germany (1983)

5. Seshadri, K., and Williams, F. A., *International Journal of Heat and Mass Transfer*, 21(2):251-253 (1978)

6. Seiser, R., Seshadri, K., Piskernik, E., and Liñán, A., *Combustion and Flame*, 122:339-349 (2000)

Appendix D: The influence of Water Vapor on the Critical Conditions of Extinction and Autoignition of Premixed Ethene Flames

M. Geieregger, R. Seiser and K. Seshadri

1 Introduction

An experimental and numerical study is carried out to characterize the influence of water vapor on critical conditions of extinction and autoignition of strained laminar premixed flames. The counterflow configuration is employed. The fuel used is ethene (C_2H_4). Water vapor has a physical as well as chemical influence on critical conditions of extinction and autoignition. Addition of water vapor lowers the temperature in reaction zone. This makes the flame (premixed and nonpremixed) easier to extinguish and more difficult to ignite. This is the physical influence of water. The chemical influence of water arises from its chaperon efficiency in three body reactions. Consider the three body reaction H + O_2 + M $\rightarrow$ HO_2 + M, where M represents any third body. This reaction is chain breaking. The concentration of the third body, C_{M} appearing in the reaction rate of this three body reaction is calculated using the relation $C_{\mathrm{M}} = [p\bar{W}/(\widehat{R}T)] \sum_{i=1}^{n} \eta_i Y_i/W_i$ where p denotes the pressure, T the temperature, $\widehat{R}$ the gas constant, $\bar{W}$ is the average molecular weight and Y_i, W_i, and η_i, are respectively the mass fraction, the molecular weight, and the chaperon efficiency of species i. In hydrocarbon air flames, the value of the chaperon efficiency of water vapor is larger than many other species in the reaction zone. This applies to many other three body reactions. Thus addition of water increases the reaction rate of three body reactions. A three body reaction that is chain breaking will make the flame easier to extinguish or more difficult to ignite when water is added to the reactant mixture.

Steady, axisymmetric, laminar flow of two counterflowing streams toward a stagnation plane is considered. Figure 1 shows a schematic illustration of the counterflow configuration employed in the present experimental and numerical study. The counterflow configuration comprises two ducts. The distance between the exits of the ducts is L. Studies on premixed systems are carried out by injecting a premixed reactant stream made up of ethene, oxygen and nitrogen from one duct, and an inert-gas stream of N_2 from the other duct. Water vapor is added to the premixed reactant stream. The mass fraction of ethene, the mass fraction of oxygen, the mass fraction of water vapor, the temperature, and the component of the flow velocity normal to the stagnation plane in the premixed reactant stream at the exit of the duct are $Y_{\mathrm{F},1}$, $Y_{\mathrm{O}_2,1}$, $Y_{\mathrm{H_2O},1}$, T_1, and V_1, respectively. The temperature, and the component of the flow velocity normal to the stagnation plane in the inert-gas stream at the exit of the duct are T_2, and V_2, respectively.

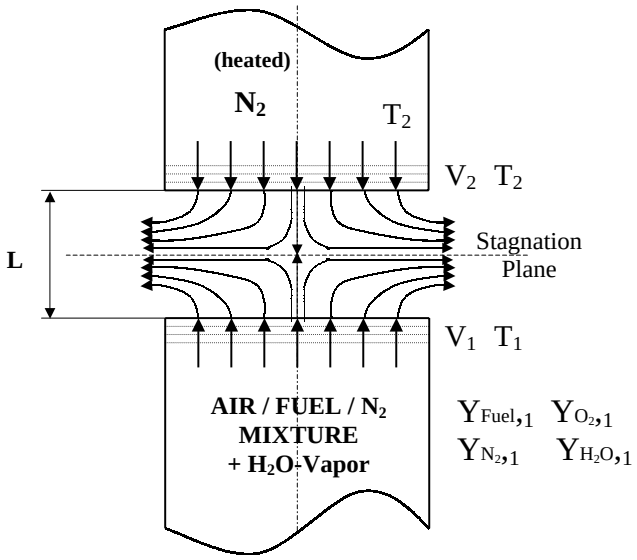

Figure 1: Schematic illustration of the counterflow configuration.

Experimental studies are conducted with the momenta of the counterflowing streams $\rho_i V_i^2$, $i = 1, 2$ kept equal to each other. Here ρ is the density. This condition ensures that the stagnation plane formed by the two streams is approximately in the middle of the region between the two ducts. The tangential components of the flow velocities at the exits of the ducts are presumed to be equal to zero (plug-flow boundary conditions). The value of the strain rate, a, defined as the normal gradient of the normal component of the flow velocity, changes from one duct exit to the other. [1]. The value of a on the inert gas side of the stagnation plane is presumed to be given by [1]

$$a_2 = \frac{2|V_2|}{L}\left(1 + \frac{|V_1|\sqrt{\rho_1}}{|V_2|\sqrt{\rho_2}}\right). \tag{1}$$

Equation (1) is obtained from an asymptotic theory where the Reynolds numbers of the laminar flows evaluated at the exits of the ducts are presumed to be large [1].

Description of Experimental and Numerical Studies

A detailed description of the burner is given elsewhere [2–5]. The flow rates of gases are measured by computer-regulated mass flow controllers. The mass flow controllers were calibrated

using a wet-test meter. The calibrated accuracy is ±1%. The gas velocities at the exit of the ducts are presumed to be equal to the ratio of their volumetric flow rates to the cross-section area of the ducts. The duct from which the inert-gas stream is injected, is equipped with a heating device, that allows the stream to be preheated. The temperature of the heated stream at the exit of the duct is measured using a Pt-Pt 13% Rh. The measured temperature are corrected for radiative heat losses assuming spherical shape of the junction, a constant Nusselt number of 2.0, and a constant emissivity of 0.2 [6]. The accuracy of the corrected temperature is expected to be better than ±25 K. Water is added to the premixed reactant stream by flowing the air through a heated bath of water. This is done in a vaporizer similar to that described in Ref. [7]. After leaving the vaporizer, the air and water vapor are mixed with ethene and nitrogen. The amount of water is calculated from the vaporizer temperature by assuming liquid vapor equilibrium. The performance of the vaporizer was tested with a hygrometer and showed above 99.0% saturation.

The experiments were carried out at a pressure $p = 1.013\,\mathrm{bar}$. The premixed reactant mixture, made up of ethene, air, water vapor and nitrogen, is characterized by the equivalence ratio, $\phi = 3Y_{\mathrm{F},1}W_{\mathrm{O}_2}/(Y_{\mathrm{O}_{2,1}}W_{\mathrm{F}})$. The adiabatic temperature, T_{ad}, can be calculated using the concentration of fuel, oxygen, nitrogen and water vapor in the premixed reactant stream. Experiments are carried out with the concentration of various species in the premixed reactant stream so chosen that the adiabatic temperature is constant. This removes the physical influence of water vapor addition on critical conditions of extinction and autoignition. This way the chemical effect of the addition of water can be studied. In the extinction experiments the temperature of the premixed reactant stream, $T_1 = 353\,\mathrm{K}$, and the temperature of the inert-gas stream, $T_2 = 298\,\mathrm{K}$ and the equivalence ratio is unity. The concentration of the reactants are so chosen that the adiabatic temperature of the premixed reactant stream are $T_{1,\mathrm{ad}} = 1823\,\mathrm{K}$ and $T_{1,\mathrm{ad}} = 1920\,\mathrm{K}$. In the extinction experiments a flame is established in the mixing layer between the premixed reactant stream and the nitrogen stream. The strain rate is increased until extinction is observed. This is done for mole fractions of water of 0.0-0.23. The strain rate at extinction is $a_{2,\mathrm{E}}$. In the autoignition experiments the temperature of the premixed reactant stream, $T_1 = 393\,\mathrm{K}$. The nitrogen stream is heated and the equivalence ratio is 0.9. Initially there is no flame present in the mixing layer. The nitrogen stream temperature T_2 is increased until autoignition is observed. The last value before ignition is recorded as the autoignition temperature $T_{2,\mathrm{I}}$. Two sets of autoignition experiments are conducted. One with $T_{1,\mathrm{ad}} = 1800\,\mathrm{K}$ and one with $T_{1,\mathrm{ad}} = 1900\,\mathrm{K}$. The strain rate a_2 was held constant at $400\,s^{-1}$. The mole fractions of water range from 0-0.18 in the 2073 K case and from 0-0.13 in the 2173 K case.

The numerical computations are carried out using a computer program called FlameMas-

ter, that was developed at RWTH-Aachen [8]. At the boundaries of the computational domain the mass flux of the reactants in the premixed reactant stream, the mass flux of nitrogen in the inert-gas stream, and their velocities are specified corresponding to those used in the experiments. Plug-flow boundary conditions are employed in the calculations. The conservation equations of mass, momentum and energy and the species balance equations used in the formulation of the numerical problem are summarized elsewhere [8, 9]. The species balance equations include thermal diffusion and the energy conservation equation includes radiative heat losses from carbon dioxide and water vapor [8]. Buoyancy is neglected. Two chemical-kinetic mechanism are employed in the numerical calculations. One mechanism, called the San Diego Mechanism, was developed at the University of California at San Diego [10]. The other mechanism called the LLNL mechanism was developed at Lawrence Livermore Laboratories [3]. The San Diego mechanism was previously employed to predict various aspects of premixed and nonpremixed combustion of ethyne (C_2H_2), ethene and ethane [11–14]. Chemical species containing three carbon atoms such as propene are included, but considered as intermediate products. The LLNL mechanism employed here was developed to predict structure, extinction and autoignition of heptane flames [3]. The LLNL was simplified by removing reactions in which species with three or more carbon atoms appear.

Results and Discussion

Figures 2 and 3 show critical conditions of extinction and autoignition. The points represent measurements and the lines are results of numerical calculation obtained using the San Diego mechanism and the LLNL mechanism. Figures 2 shows the strain rate at extinction, $a_{2,\mathrm{E}}$, as a function of the mole fraction of water vapor in the premixed reactant stream, $X_{\mathrm{H_2O},1}$. Experimental data and results of numerical calculation with LLNL mechanism show that $a_{2,\mathrm{E}}$ decreases with increasing values of $X_{\mathrm{H_2O},1}$. Numerical results obtained using the LLNL mechanism agrees well with the experimental data. Numerical calculations with the San Diego mechanism show $a_{2,\mathrm{E}}$ to slightly increase with increasing values of $X_{\mathrm{H_2O},1}$. At a given value of $X_{\mathrm{H_2O},1}$, the value of $a_{2,\mathrm{E}}$ calculated using the San Diego Mechanism is higher than the measurements.

Figure 3 shows the temperature of the inert-gas stream at autoignition, $T_{2,\mathrm{I}}$, as a function of the mole fraction of water vapor in the premixed reactant stream, $X_{\mathrm{H_2O},1}$. Experimental data and results of numerical calculation with LLNL mechanism show that $T_{2,\mathrm{I}}$ increases with increasing values of $X_{\mathrm{H_2O},1}$. Numerical calculations with the San Diego mechanism show $T_{2,\mathrm{I}}$ to slightly decrease with increasing values of $X_{\mathrm{H_2O},1}$. Thus experimental data and numerical calculation with the LLNL in Figs. 2 and 3 show that the flame gets weaker with addition of water, whereas numerical calculations with the San Diego mechanism show that the flame

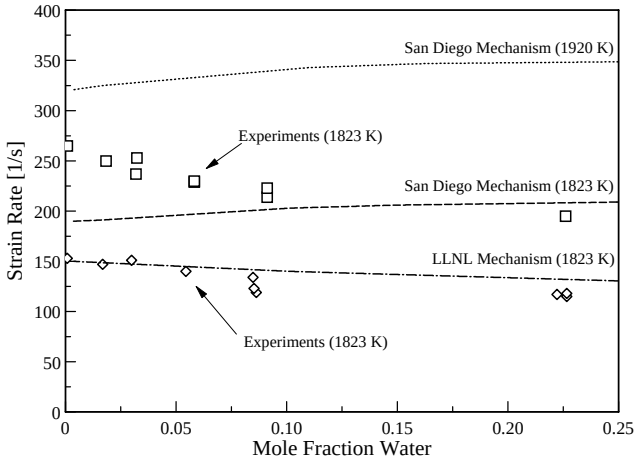

Figure 2: The strain rate at extinction, $a_{2,\mathrm{E}}$, as a function of the mole fraction of water vapor in the premixed reactant stream, $X_{\mathrm{H_2O},1}$. The points represent measurements and the lines are results of numerical calculation using the San Diego mechanism and the LLNL mechanism. Experiments and calculations are carried out keeping the adiabatic flame temperature constant at 1823 K and 1920 K, respectively.

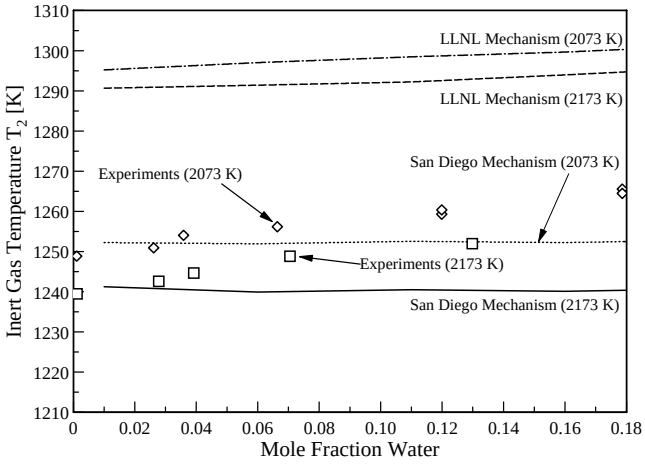

Figure 3: The temperature of the inert-gas stream at autoignition, $T_{2,\mathrm{I}}$, as a function of the mole fraction of water vapor in the premixed reactant stream, $X_{\mathrm{H_2O},1}$. The points represent measurements and the lines are results of numerical calculation using the San Diego mechanism and the LLNL mechanism. Experiments and calculations are carried out keeping the adiabatic flame temperature constant at 2073 K and 2173 K, respectively. The equivalence ratio is 0.9.

gets stronger with addition of water.

Calculations with the San Diego mechanism show that among the three body reactions, the elementary reactions $H + O_2 + M_6 = HO_2 + M_6$, and $HCO + M_4 = H + CO + M_4$ play key roles in influencing critical conditions of extinction and autoignition. In the San Diego mechanism the chaperon efficiency of water vapor is $M_6 = 7$, and $M_4 = 12.0$ respectively. Figure 4 shows the influences of these elementary reactions on critical conditions of extinction.

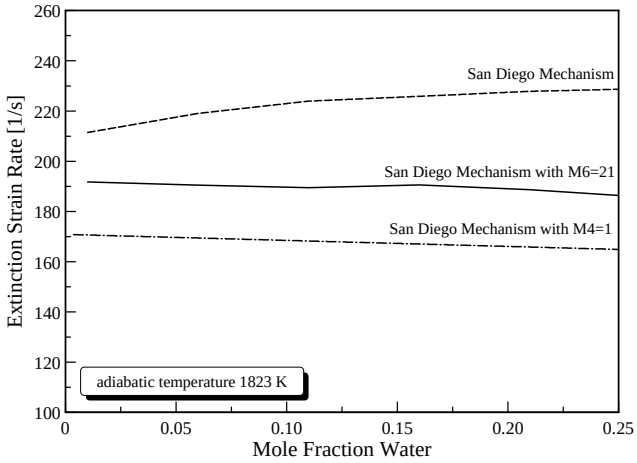

Figure 4: Numerical calculated values of the strain rate at extinction, $a_{2,\mathrm{E}}$, as a function of the mole fraction of water vapor in the premixed reactant stream, $X_{\mathrm{H_2O},1}$. The calculations were performed using the San Diego mechanism. The figure shows the influences of the elementary reactions $H + O_2 + M_6 = HO_2 + M_6$, and $HCO + M_4 = H + CO + M_4$

Figure 4 shows that value of $a_{2,\mathrm{E}}$ decreases with increasing mole fraction of water vapor in the premixed reactant stream if the value of M_6 is increased from 7 to 21, or if the value of M_4 is decreased from 12 to 1.

Figure 5 shows that the values of the temperature of the inert-gas stream at autoignition, $T_{2,\mathrm{I}}$ increases with increasing mole fraction of water in the the premixed reactant stream if the M_6 is increased from 7 to 21, or if the value of M_4 is decreased from 12 to 1. Similar results are obtained if the value of chaperon efficiency in all three body reactions are presumed to be unity.

The elementary reaction $H + O_2 + M_6 = HO_2 + M_6$ is chain breaking. Therefore increasing the rate of this reaction makes the flame easier to extinguish and harder to ignite. On the other hand the elementary reaction $HCO + M_4 = H + CO + M_4$ produces radicals. Therefore increasing the rate of this reaction makes the flame harder to extinguish and easier to ignite.

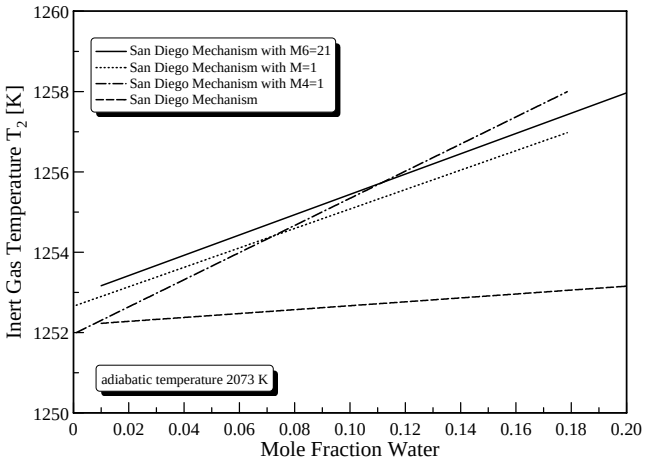

Figure 5: Numerical calculated values of the temperature of the inert-gas stream at autoignition, $T_{2,\mathrm{I}}$, as a function of the mole fraction of water vapor in the premixed reactant stream, $X_{\mathrm{H_2O},1}$. The calculations were performed using the San Diego mechanism. The figure shows the influences of the elementary reactions H + O_2 + M_6 = HO_2 + M_6, and HCO + M_4 = H + CO + M_4

This is consistent with the results of numerical calculations in Figs. 4 and 5.

References

[1] K. Seshadri and F. A. Williams. Laminar flow between parallel plates with injection of a reactant at high Reynolds number. *International Journal of Heat and Mass Transfer*, 21(2):251–253, 1978.

[2] R. Seiser, L. Truett, D. Trees, and K. Seshadri. Structure and extinction of non-premixed *n*-heptane flames. *Proceedings of the Combustion Institute*, 27:649–657, 1998.

[3] R. Seiser, H. Pitsch, K. Seshadri, W. J. Pitz, and H. J. Curran. Extinction and autoignition of *n*-heptane in counterflow configuration. *Proceedings of the Combustion Institute*, 28:2029–2037, 2000.

[4] R. Seiser, K. Seshadri, E. Piskernik, and A. Liñán. Ignition in the viscous layer between counterflowing streams: Asymptotic theory with comparison to experiments. *Combustion and Flame*, 122:339–349, 2000.

[5] R. Seiser, L. Truett, D. Trees, and K. Seshadri. Nonpremixed and premixed extinction and autoignition of C_2H_4, C_2H_6, C_3H_6, and C_3H_8. *Proceedings of the Combustion Institute*, 29:in press, 2002.

[6] T. Weißweiler. Measurements of stable species and soot volume fraction in a propane-air counterflow diffusion flame. Diploma thesis, Institut für Allgemeine Mechanik, RWTH Aachen, Aachen, Germany, 1994.

[7] R. Seiser. *Nonpremixed Combustion of Liquid Hydrocarbon Fuels*. Ph.D thesis, Technical University of Graz, 2000.

[8] H. Pitsch. Entwicklung eines Programmpaketes zur Berechnung eindimensionaler Flammen am Beispiel einer Gegenstromdiffusionsflamme. Master's thesis, RWTH Aachen, Germany, 1993.

[9] N. Peters. Flame calculations with reduced mechanisms - an outline. In N. Peters and B. Rogg, editors, *Reduced Kinetic Mechanisms for Applications in Combustion Systems*, volume m15 of *Lecture Notes in Physics*, chapter 1, pages 1–13. Springer-Verlag, Heidelberg, 1993.

[10] The San Diego Mechanism. http://maeweb.ucsd.edu/combustion/.

[11] B. Varatharajan and F. A. Williams. Chemical-kinetic descriptions of high-temperature ignition and detonation of acetylene-oxygen-diluent systems. *Combustion and Flame*, 124:624–645, 2001.

[12] M. M. Y. Waly, S. C. Li, and F. A. Williams. Structures of non-sooting counterflow diluted acetylene-air flames. *Proceedings of the Combustion Institute*, 28:2005–2012, 2000.

[13] B. Varatharajan and F. A. Williams. Ethylene ignition and detonation chemistry, part 2: Ignition histories and reduced mechanisms. *Journal of Propulsion and Power*, 18:352–362, 2002.

[14] M. M. Y. Waly, S. C. Li, and F. A. Williams. Experimental and numerical studies of two-stage ethane-air flames. *Journal of Engineering for gas Turbines and Power*, 122(4):651–658, 2000.